

# **Material Performance of Fully-Ceramic Micro-Encapsulated Fuel Under Selected LWR Design Basis Scenarios: Final Report**

Brian Boer  
R. Sonat Sen  
Michael A. Pope  
Abderrafi M. Ougouag

September 2011



The INL is a U.S. Department of Energy National Laboratory operated by Battelle Energy Alliance

**INL/EXT-11-23313  
FCR&D-2011-000338**

# **Material Performance of Fully-Ceramic Micro-Encapsulated Fuel Under Selected LWR Design Basis Scenarios: Final Report**

**Brian Boer  
R. Sonat Sen  
Michael A. Pope  
Abderrafi M. Ougouag**

**September 2011**

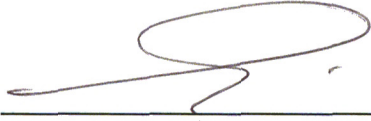
**Idaho National Laboratory  
Fuel Cycle Research & Development  
Idaho Falls, Idaho 83415**

**<http://www.inl.gov>**

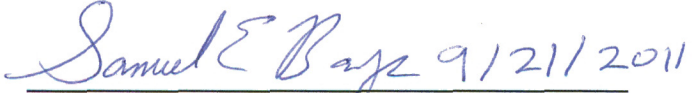
**Prepared for the  
U.S. Department of Energy  
Office of Nuclear Energy  
Under DOE Idaho Operations Office  
Contract DE-AC07-05ID14517**



**Co-Authors:**

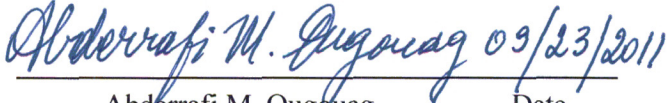
  
\_\_\_\_\_  
R. Sonat Sen For Brian Boer and      09/21/2011  
Michael A. Pope                                  Date

**Reviewed by:**

  
\_\_\_\_\_  
Samuel E. Bays                                  9/21/2011  
Date

**Concurred by:**

Co-Author and Work Package Manager

  
\_\_\_\_\_  
Abderrafi M. Ougouag                          09/23/2011  
Date

*Performance of Fully-Ceramic Micro-Encapsulated Fuel Under Selected Design Basis Accident Scenarios: Final Report*

September 2011

iv

---

## CONTENTS

ACRONYMS.....	viii
Summary .....	ix
1. Introduction .....	1
1.1 Objective and scope .....	1
1.2 Description of the FCM fuel .....	2
2. Operating conditions of the FCM fuel.....	3
2.1 Fluence level in the FCM fuel.....	3
2.2 Thermal model pin-type fuel containing coated particles .....	3
3. Material Properties of fuel and coatings at LWR-DB conditions.....	5
3.1 SiC Thermal Conductivity .....	5
3.2 Swelling and creep of SiC under neutron radiation .....	6
3.3 Swelling of PyC under DB-LWR conditions.....	7
4. Description of the PASTA code .....	11
5. Description Of the neutronic analysis using the DRAGON code .....	13
6. Stress analysis and fuel performance of FCM fuel.....	14
6.1 Performance of the reference design under Normal operating conditions.....	14
6.2 Impact of the kernel size on the fuel performance .....	18
6.3 Impact of the SiC-matrix on the particle performance.....	20
7. Optimization of the FCM coated particle design.....	24
7.1 Impact of design modifications on performance.....	24
7.2 Optimization of the buffer and OPyc thickness .....	26
7.3 Fuel perormance at Loss of coolant accident conditions .....	28
8. Conclusions .....	31
9. Recommendations for experimental work regarding the performance of FCM fuel.....	33
References.....	35

## FIGURES

Figure 1. Fast ( $E > 0.1$ MeV) fluence level as a function of the fuel burnup calculated with the DRAGON code.....	3
Figure 3. Swelling of SiC as a function of temperature for several levels of neutron damage [11]. .....	6

Figure 4. Dimensional change of PyC as a function of the fast fluence for the radial and tangential directions in two temperature ranges (600-800°C and 800-1000°C), [12].	7
Figure 5. Dimensional change of PyC as a function of the fast ( $>E_c = 0.18$ MeV) fluence for the radial and tangential directions for high density (isotropic and slightly anisotropic) and low density graphite, [16].	8
Figure 8. Overview of the DRAGON-PASTA calculation procedure for fuel performance analysis.	12
Figure 9. Pressure in the buffer layer of the coated from Xe and Kr release from the kernel.	15
Figure 10. Tangential stresses in the coating layers during irradiation of the particle (with reference dimensions).	15
Figure 11. Tangential stress in the SiC layer and the pressure in the carbon buffer layer as a function of the burnup for the particle with the reference coating dimensions.	16
Figure 12. Failure probability as a function of the burnup for the particle with the reference coating dimensions.	16
Figure 13. Tangential stress in the SiC layer as a function of the burnup for the particle with the reference coating dimensions with the percentage of fission gas release as a parameter.	17
Figure 14. Failure probability as a function of the burnup for the particle with the reference coating dimensions with the fission gas release fraction as a parameter.	17
Figure 16. Tangential stress in the SiC layer as a function of the kernel diameter calculated with the PASTA code.	19
Figure 17. Schematic overview of the coating layers surrounding the FCM fuel kernel, which are embedded in the SiC-matrix.	20
Figure 20. Failure probabilities of the various particle designs (presented in Table 6) at burnup levels of 500, 600 and 700 MWd/kg iHM.	26
Figure 21. Tangential stresses in the coating layers and the buffer pressure as a function of the burnup for the particle with a buffer thickness of 120 micron and an OPyC thickness of 10 micron.	27
Figure 22. Failure probability as a function of the burnup for the particle with a buffer thickness of 120 micron and a OPyC thickness of 10 micron, with the fission gas release fraction as a parameter.	28
Figure 23. Coating stresses for a particle that experiences a LOCA transient at the end of its life-time in which the temperature of the particle is increased with 400 K.	29
Figure 24. SiC-coating stresses for a particle that experiences a LOCA transient for various points in its life-time both a temperature increase of 200 K and of 400 K.	29

## TABLES

Table 1. Dimensions of the coating layers in the FCM fuel design.	2
Table 2. Composition of the Deep-Burn fuel.	2
Table 3. Conditions of the FCM fuel during normal operation.	14

***Performance of Fully-Ceramic Micro-Encapsulated Fuel Under Selected Design Basis Accident Scenarios: Final Report***

September 2011

vii

---

Table 4. Coating material properties taken from [11], [15], [16]. .....	14
Table 5. Maximum tensile stress in the SiC layer for a particle surround by SiC-matrix material. ....	21
Table 6. Reference and modified particle designs and their TRU loading per pellet (deviations from the reference design are indicated in grey). .....	24
Table 7. Results of PASTA and DRAGON calculations for the reference and modified particle designs. ....	25
Table 8. Particle performance for several combinations of the buffer and OPyC layer thicknesses. ....	27



## ACRONYMS

BAF	Bacon Anisotropy Factor
DB	Deep-Burn
DOE	Department of Energy
FCM	Fully Ceramic Microencapsulated (fuel)
FIMA	fissions per initial metal atom
iHM	initial Heavy Metal
IMF	Inert Matrix Fuel
INL	Idaho National Laboratory
IPyC	inner pyrolytic carbon
LWR	light water reactor
NEA	Nuclear Energy Agency
OECD	Organization for Economic Co-operation and Development
OPyC	outer pyrolytic carbon
RHRS	reactor heat removal system
SiC	silicon carbide
TRISO	tri-isotopic
TRU	transuranic

## SUMMARY

The extension of the use of Deep-Burn (DB) coated particle fuel envisaged for use in High Temperature Reactors (HTRs), to existing Light Water Reactors (LWRs) has been investigated. In this case the TRISO coated fuel particles are used in Fully-Ceramic Microencapsulated (FCM) fuel within a SiC matrix rather than the graphite matrix typically used in HTRs. TRISO fuel particles have been well characterized for uranium fueled HTRs. However, LWRs exhibit different operating conditions as compared to HTRs in terms of temperature, neutron energy spectrum, fast fluence levels and power density. Furthermore, the time scales of transient core behavior during accidents are in general much shorter in LWRs.

The Particle STress Analysis (PASTA) code has been updated to allow for the stress analysis of coated particle FCM fuel. The code extension enables the automatic use of the neutronic data (burnup, fast fluence as a function of the irradiation time) that is generated with the DRAGON neutronics code. Furthermore, an input option for automatic evaluation of a temperature increase during anticipated transients has been added to the code. A new thermal model for FCM was incorporated in the code, as well as updated correlations for the pyrocarbon coating layers that can estimate dimensional change at the high fluence levels attained in LWR DB fuel.

From the analyses of the FCM fuel with the updated PASTA code under nominal and accident conditions it was found that:

- The stress levels in the SiC-coating are low in general for low Fission Gas Release (FGR) fractions of several percent, which are based on data for fission gas diffusion in UO<sub>2</sub> kernels. However, taking in mind the high burnup level of LWR-DB, the FGR fraction is more likely to be in the range of 50 -100 %, similar to Inert Matrix Fuels (IMFs). For this range the predicted stresses and failure fractions of the SiC-coating are high for the reference particle design (500 μm kernel diameter, 100 μm buffer, 35 μm IPyC, 35 μm SiC, 40 μm OPyC).

A conservative case in which the FGR fraction is assumed to be 100 %, the fuel temperature 900 K and a fuel burnup of 705 MWd/kg (77 % FIMA) would result in a failure probability of  $8.0 \times 10^{-2}$ . For a 'best-estimate' FGR-fraction of 50 % and a more modest burnup target level of 500 MWd/kg the failure probability drops below a value of  $2.0 \times 10^{-5}$ , which is the typical performance of TRISO fuel made under the German HTR research program in the past.

- In an optimization study on the particle design it was found that the performance can be improved if the buffer size is increased from 100 μm to 120 μm, while reducing the OPyC layer. The presence of the latter layer does not provide much benefit at high burnup levels (and fast fluence levels). Normally the shrinkage of the OPyC would result in a compressive force on the SiC-coating, which is advantageous. However, at high fluence levels the shrinkage is expected to turn into swelling, resulting in the opposite effect. This situation is however different when the SiC-matrix, in which the particles are embedded, is also considered. In that case, the OPyC swelling can result in a positive (compressive force on the SiC-coating) effect. The outward displacement of the OPyC outer surface is inhibited by the presence of the SiC-matrix. Taking some credit for this effect by adopting a 5 μm, SiC-matrix layer, the optimized particle (100 μm buffer and 10 μm OPyC), gives a failure probability of  $1.9 \times 10^{-4}$  for conservative conditions.
- During a LOCA transient, assuming a core re-flood in 30 seconds, the temperature of the coated particle can be expected to be about 200 K higher than nominal temperature of 900K. For this event the particle failure fraction for a conservative case was  $1.0 \times 10^{-2}$ , for the optimized particle design. For a FGR-fraction of 50 % this value reduces to  $6.4 \times 10^{-4}$ .

- To allow for future deployment of FCM fuel the following topics, in order of importance, are recommended for further investigation by computer modeling and experimental work:

### **1. Dimensional change and creep of PyC material**

From a literature survey it was found that experimental data regarding the dimensional change and creep under radiation of PyC is relatively scarce. For neutron fluence levels between  $8.0 \times 10^{21}$  and  $30 \times 10^{21} \text{ cm}^{-2}$  ( $E > 0.1 \text{ Mev}$ ), which are relevant for FCM fuel, there is no data available in literature. An experimental program for the quantification of PyC dimensional change is therefore highly recommended.

### **2. Fission gas release from the FCM kernel**

In comparison with HTR TRISO fuel kernels, the irradiation conditions of the FCM fuel kernel are very different. The temperature of the kernel is lower ( $T_{\text{max,FCM}}=900\text{K}$ ,  $T_{\text{max,HTR}}= 1500 \text{ K}$ ), while the maximum attained fluence levels are higher ( $\Phi_{\text{max,FCM}}=30 \times 10^{21} \text{ cm}^{-2}$ ,  $\Phi_{\text{max,HTR}}= 8.0 \times 10^{21} \text{ cm}^{-2}$ ). The first would typically result in a lower fission gas release from the kernel while the latter might induce a high fractional release. Furthermore, the FCM fuel kernel contains a SiC-getter, which could ‘immobilize’ the fission gases resulting in a reduced fission gas release fraction.

It is unclear whether the combined effects would result in a higher or lower FGR as compared to typical HTR fuel kernels. Experimental work regarding FGR is key for the determination of the fuel performance of FCM fuel.

### **3. Mechanical integrity of the OPyC coating layer and SiC-matrix**

In the stress analysis it was found that the presence of the SiC-matrix can induce high stresses in the coating layers of the particle due to dimensional change of the OPyC layer. This phenomenon is not encountered in HTR TRISO fuel, since in that case a ‘softer’ graphite-matrix is used. It is therefore recommended that in a possible future irradiation experiment of FCM fuel, that the coated particles are embedded in a SiC-matrix.

Furthermore, the packing fraction of FCM is high (~44%) as compared to HTR fuel. Therefore, a given particle will have one or more neighboring particles within close proximity. This could induce further stress effects. It is therefore of key importance that the FCM coated fuel particles are embedded in a SiC-matrix with high packing fraction during a future irradiation testing campaign.

Next to the experimental work itemized above, the incorporation in the PASTA code of the updated correlations and a re-evaluation of the fuel performance is recommended.

The following topics, in order of importance, are recommended for further investigation in computer modeling:

### **4. Impact of the SiC-matrix and neighboring particles on the coating stress**

Modeling of three-dimensional stress effects by neighboring particles and SiC-matrix to quantify the impact on the fuel performance is recommended. The results of 3D (finite element) modeling of coated particle fuel in matrix material could be used to update the boundary conditions of the (1D) stress analysis in PASTA. Next to this modification direct coupling with another code,

typically a finite element code, would also allow for the evaluation of matrix effects. In any case, three-dimensional modeling of coated particle fuel in matrix material is recommended.

**5. Coupling of the PASTA code with fuel performance model for pin-type fuel**

In order to treat the entire fuel geometry (coated particle, pellet, gap, cladding) the PASTA code could be coupled to fuel performance codes that are dedicated to pin-type fuel, such as TRANSURANUS or FRAPCON. This would allow for the re-evaluation of the current envisaged FCM pin-type fuel.

*Performance of Fully-Ceramic Micro-Encapsulated Fuel Under Selected Design Basis Accident Scenarios: Final Report*

September 2011

xii

---

## **1. INTRODUCTION**

The Deep Burn (DB) concept [1] is under investigation for feasibility, safety, effectiveness, and efficiency. The concept was created for the purpose of destroying the inventory of plutonium (Pu) and Minor Actinides (MA) from legacy and future used Light Water Reactor (LWR) fuel. The DB concept could be implemented potentially within any reactor platform, but has been primarily considered in the past for High Temperature gas-cooled Reactors (HTRs). The TRISO-coated particle fuel that is used in this type of reactor has shown excellent performance at the high burnup levels required for the DB concept.

The extension of the use of DB coated particle fuel to existing LWRs has been investigated. In this case the TRISO coated fuel particles are used in Fully-Ceramic Microencapsulated (FCM) fuel within a SiC matrix [2] rather than the graphite matrix typically used in HTRs. Although the TRISO fuel particles have been well characterized, LWRs exhibit different operating conditions as compared to HTRs in terms of temperature, neutron energy spectrum, fast fluence levels and power density. Furthermore, the time scales of transient core behavior during accidents are in general much shorter in LWRs (i.e., more severe). Therefore, the performance of the coated particle fuel has to be re-analyzed for these new conditions. The assumptions for the models and the correlations for the material properties of the coating layers as well as the matrix material have to be re-evaluated. Furthermore, the fuel performance during typical LWR transient operation must be analyzed.

### **1.1 OBJECTIVE AND SCOPE**

The objectives of the work presented in this report are as follows:

1. To perform scoping studies of the performance of TRISO particles in LWR FCM fuel during static and transient conditions typical of LWR performance. From these analyses necessary improvements of the existing methods and codes, such as the PArticle STress Analysis code (PASTA) have been identified.
2. Evaluation of the performance analysis of FCM under DB LWR conditions with the updated PASTA code [3]. This incorporates model development and incorporation into the PASTA code in support of modeling Fully Ceramic Microencapsulated fuel (FCM) and related stress fields within TRISO particles, and intervening matrix. Apply the new models to evaluate failure rate of TRISO particles and influence of matrix changes on said failure rate.
  - a. Initiate making the transient evaluation automatic by modifying the PASTA code; the preliminary results are expected to be computed by manual coupling of the various physics not already coupled within the PASTA code
  - b. Incorporation of correlations for the material properties of FCM fuel in the PASTA code to be used for stress analysis.
  - c. Implementation of a thermal model for FCM in the PASTA code.
  - d. Stress analysis of the coated particle fuel with the PASTA code. The boundary conditions (fluence, power, burnup and fission product formation) for the analyses have to be provided by neutronics analysis (DRAGON).
3. Identification of possible optimization of the coated particle design for FCM fuel and LWR conditions.

## 1.2 DESCRIPTION OF THE FCM FUEL

The FCM fuel adopts the “rod bundle” geometry of light water reactors [2]. The configuration that is considered here is similar to that of the EPR design [4]. However, in contrast with the typical uranium dioxide (or MOX) fuel pellets used in the EPR fuel rod, the FCM fuel uses TRISO-coated fuel particles within a SiC-matrix. The fuel particles are currently assumed to occupy *up to* 48% of the volume, while the remainder is occupied by the SiC matrix.

The dimensions of the coated particles are given in Table 1. In the fuel kernel a SiC getter is used to prevent the production of CO by chemically reacting free oxygen, which is formed during irradiation of the fuel. The isotopic composition of the Pu and Minor Actinide (MA) fuel proper is given in Table 2.

**Table 1. Dimensions of the coating layers in the FCM fuel design.**

Layer	Thickness (μm)
Kernel (TRU-O <sub>1.8</sub> (SiC) <sub>0.6</sub> )	350*
Buffer	100
IPyC	35
SiC	35
OPyC	40

\* Kernel diameter.

**Table 2. Composition of the Deep-Burn fuel.**

Isotope	Fraction (wt. %)
<sup>237</sup> Np	6.8
<sup>238</sup> Pu	2.9
<sup>239</sup> Pu	49.38
<sup>240</sup> Pu	23
<sup>241</sup> Pu	8.8
<sup>242</sup> Pu	4.9
<sup>241</sup> Am	2.8
<sup>242m</sup> Am	0.02
<sup>243</sup> Am	1.4

The remainder of this report presents the analysis of the above presented FCM fuel in LWR reactors. In the following sections the fuel operating conditions (Section 2) and important material properties of the coating materials (Section 3) previously analyzed for HTR conditions are re-evaluated for LWR conditions. The performance of the fuel at these new conditions is analyzed using the PASTA stress analysis code (Section 4), which has been modified to read the output of the DRAGON neutronics code (Section 5). The results of the fuel performance analysis are presented in Section 6. The optimization of the coated particle and its performance under design basis accident conditions is given in Section 7. The

final two sections of the document present the conclusion (Section 8) and recommendations (Section 9) regarding possible future computational and experimental work.

## 2. OPERATING CONDITIONS OF THE FCM FUEL

This section presents the typical fluence levels and temperatures of FCM fuel during irradiation in a LWR.

### 2.1 FLUENCE LEVEL IN THE FCM FUEL

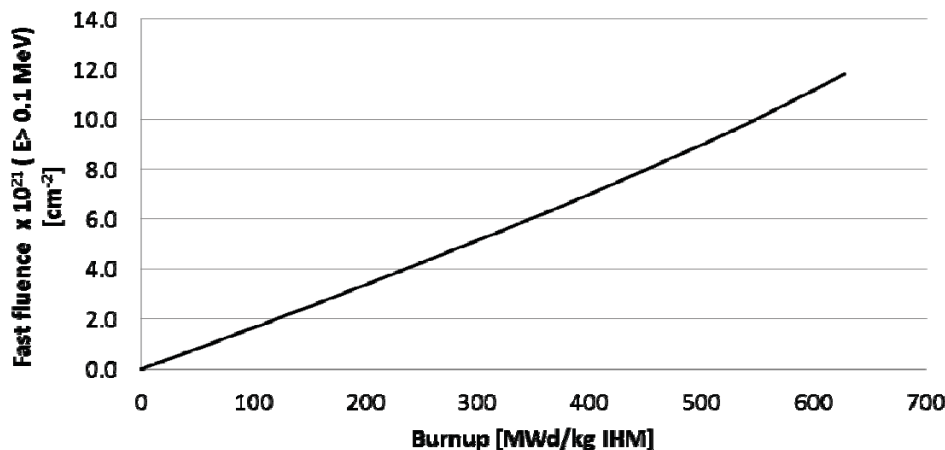


Figure 1. Fast ( $E > 0.1$  MeV) fluence level as a function of the fuel burnup calculated with the DRAGON code.

In Figure 1 the fast fluence level as a function of the burnup for the FCM fuel is presented. The fluence level has been calculated using the DRAGON code [5]. The analysis shows that for the same discharge burnup of 500-700 MWd/kg iHM the fast fluence level attained in the DB-LWR is about a factor of two higher than for DB fuel irradiated in a DB-HTR [6].

### 2.2 THERMAL MODEL PIN-TYPE FUEL CONTAINING COATED PARTICLES

The temperature in a fuel pin with dispersed coated fuel particles can be estimated from the power density and the temperature at the boundary. For the effective conductivity of a fuel pin,  $K_{eff}$ , a Maxwell-Garnett [7] model is adopted, which takes into account both the coated particles and the SiC matrix:

$$K_{eff} = \lambda_m \left( \frac{\lambda_i(1+2\alpha) - \lambda_m(2\alpha-2)}{\lambda_m(2+\alpha) + \lambda_i(1-\alpha)} \right) \quad (1)$$

in which  $\lambda_i$  is the conductivity of the fuel kernel,  $\lambda_m$  is the conductivity of the SiC matrix and  $\alpha$  is the volume fraction of fuel kernels in the matrix. It is assumed that the coating layers of the particle, consisting of SiC and carbon, have roughly the same conductivity as the SiC matrix. It is noted that with a packing fraction of 50% coated particles in the fuel pin and the radii of the kernel and coated particle (kernel and coating layers) at 175  $\mu\text{m}$  and 390  $\mu\text{m}$ , respectively,  $\alpha$  takes the value 0.045. Assuming that



the kernel has a conductivity of 2 W/m/K and the SiC matrix a conductivity of 20 W/m/K, there results an effective conductivity for the fuel pin of 18 W/m/K.

The temperature drop over the fuel pin can be calculated with:

$$\Delta T_{fuel} = \frac{q'}{4\pi K_{eff}} \quad (2)$$

With a linear power,  $q'$ , of 500 W/cm, a temperature drop of 221 K is found. This is small compared to the typical temperature drop in a 'normal' UO<sub>2</sub> fuel pellet, which is around 1400 K. The temperature drop over the gap, Zr-cladding and coolant at this power are 200 K, 80 K and 20 K, respectively (see for example [8]). At a typical coolant temperature of 580 K the LWR-DB fuel centerline temperature is 1200 K. Note that a linear power of 500 W/cm is a conservative value, since the average linear power in an EPR type reactor of 4500 MW with 241 x 265 pins is 170 W/cm. The latter linear power would result in a center fuel temperature of 791 K.

The power per kernel (0.16 W for 350 μm kernel and PF=48%) in the DB-LWR fuel is significantly higher than in the DB-HTR (0.06 W). Therefore the temperature difference over the kernel itself could become significant. Furthermore, formation of a gap between the buffer layer and the IPyC could further increase the temperature difference between the kernel and the SiC matrix. The temperature difference between the center and the outer surface of the kernel is given by:

$$\Delta T_{kern} = \frac{q'''_{kern} R_{kern}^2}{6K_{kern}} \quad (3)$$

in which  $q'''$  is volumetric power,  $R$  is radius, and the subscript *kern* refers to the kernel properties. Assuming a power density and a thermal conductivity, respectively, of 7.0 GW/m<sup>3</sup> and 2 W·m<sup>-1</sup>·K<sup>-1</sup> for the kernel leads to a temperature difference of 18 K. The temperature difference over the gap can be calculated with [9],

$$\Delta T_{gap} = \frac{q'''_{kern} R_{kern}^3}{3K_{gap}} \left( \frac{1}{R_{buf,0} - t_{gap}} - \frac{1}{R_{buf,0}} \right) \quad (4)$$

where  $K_{gap}$  is the effective gap thermal conductivity and  $R_{buf}$  is the outer radius of the buffer layer. The gap radius ( $t_{gap}$ ) in this equation is calculated from the volume change of the buffer with [9]:

$$t_{gap} = R_{buf,0} - \sqrt[3]{R_{kern}^3 + \frac{(1 + \Delta V) V_{buf,0}}{4/3 \pi}} \quad (5)$$

where  $V_{buf}$  is the initial buffer volume and  $\Delta V$  is the change in buffer volume. A gap thickness of 18 μm is found, assuming that the buffer volume decreases by 25%. This leads to a temperature difference over the gap (with  $K_{gap} = 3.2 \times 10^{-2}$  W·m<sup>-1</sup>·K<sup>-1</sup>) (see Ref. 10) of 102 K. The average kernel centerline temperature at the pin center can therefore be expected to be around 900 K.

### 3. MATERIAL PROPERTIES OF FUEL AND COATINGS AT LWR-DB CONDITIONS

#### 3.1 SiC THERMAL CONDUCTIVITY

The unirradiated (phonon) conductivity of SiC as a function of the temperature [K] can be described with the following correlation ( $T > 300\text{K}$ ) (Figure 2, “Highly pure and dense single-/poly-crystals”) [11]:

$$K_{non,irr} = \left( -3.0 \times 10^{-4} + 1.05 \times 10^{-5} T \right)^{-1} \quad (6)$$

At room temperature, this correlation gives a conductivity of 350 W/m/K. Neutron irradiation introduces defects in the SiC material resulting in an increase of the thermal resistance ( $1/K_{rd}$ ) [11]. The conductivity of irradiated SiC can then be described as:

$$K_{irr} = \left( \frac{1}{K_{non,irr}} + \frac{1}{K_{rd}} \right)^{-1} \quad (7)$$

The thermal resistance ( $1/K_{rd}$ ) due to radiation at a temperature range of 750 – 850°C is 0.031 and 0.040 at fast ( $E > 0.1$  MeV) neutron fluence levels of  $1.0 \times 10^{21}$  and  $5.0 \times 10^{21}$  n/cm<sup>2</sup>, respectively. This results in conductivity values between 20 and 25 W/m/K at these temperatures and fluence levels.

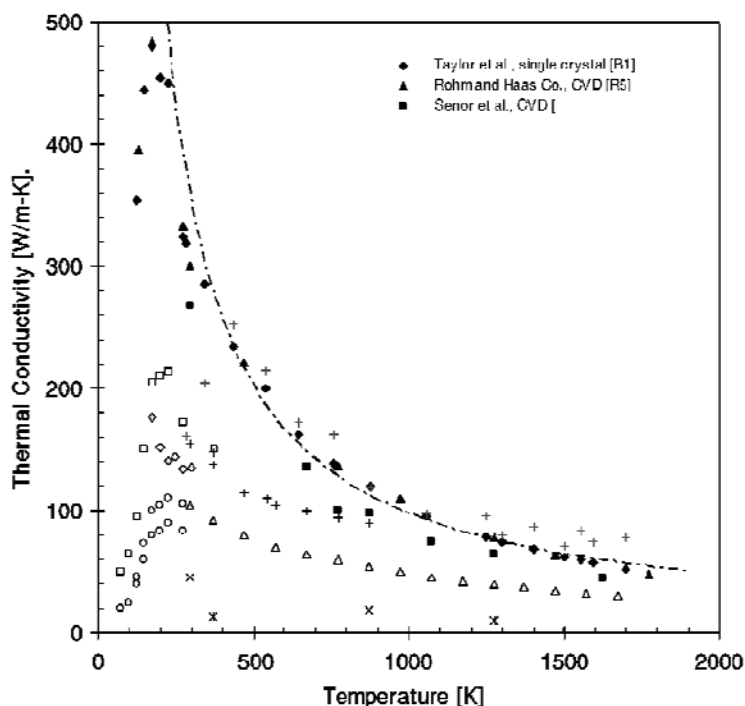


Figure 2. Thermal conductivity of unirradiated SiC as a function of temperature for several types of SiC [11].

### 3.2 SWELLING AND CREEP OF SiC UNDER NEUTRON RADIATION

Since SiC is also used as the matrix material, this dimensional change could introduce stress effects in the FCM fuel. In Figure 3, the swelling behavior of SiC is shown as a function of the temperature. It can be seen that the SiC material exhibits some swelling for DB-LWR conditions, but that its magnitude is typically below 1 % for LWR-DB conditions. Therefore, swelling of the SiC has been neglected in the stress analysis.

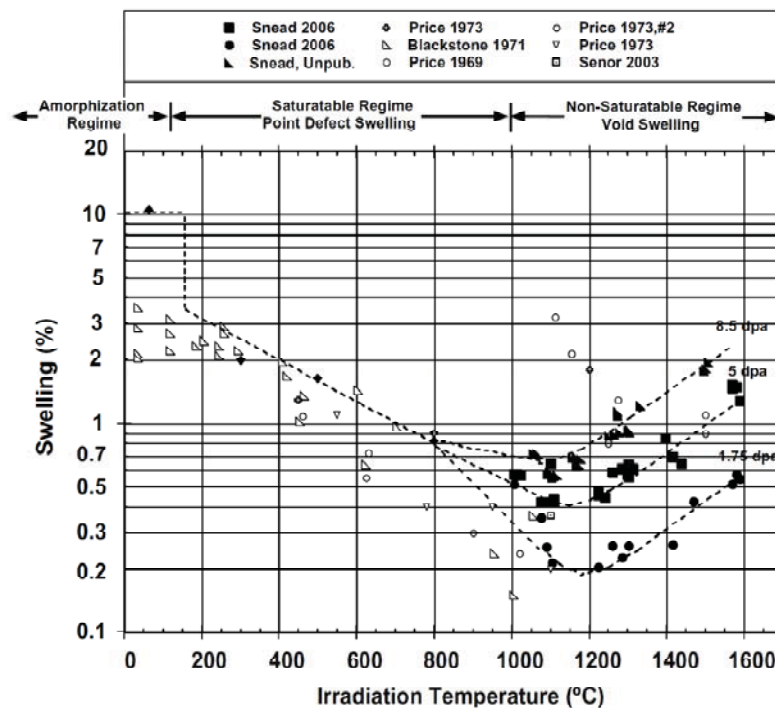


Figure 3. Swelling of SiC as a function of temperature for several levels of neutron damage [11].

### 3.3 SWELLING OF PYC UNDER DB-LWR CONDITIONS

Figure 4 shows the dimensional change of PyC material as a function of the fast fluence for two temperature ranges (600-800°C and 800-1000°C), [12]. It can be seen that the material exhibits more dimensional change for the higher temperature range. Therefore it can be expected that the compressive stress that the PyC layer induces on the SiC is less in the DB-LWR (lower temperature range) than in the DB-HTR.

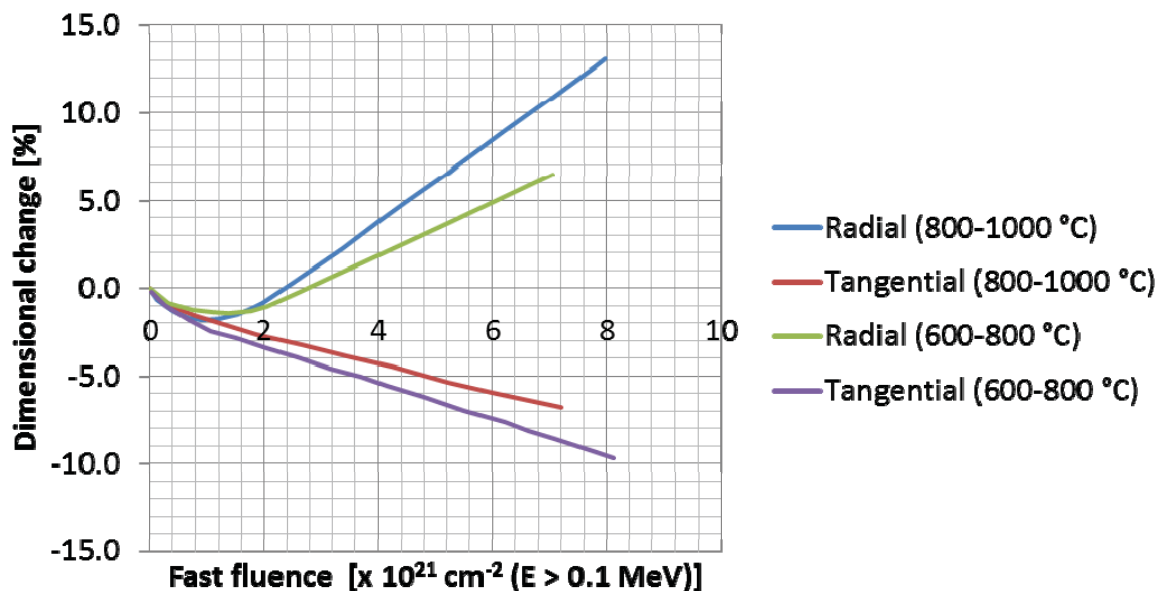


Figure 4. Dimensional change of PyC as a function of the fast fluence for the radial and tangential directions in two temperature ranges (600-800°C and 800-1000°C), [12].

Based on analysis with the DRAGON neutronics the anticipated fast fluence at high burnup levels of 600-700 MWd/kg iHM are  $18 - 35 \times 10^{21} \text{ n/cm}^2$ , respectively. The available experimental data for PyC (density range  $1.80 - 1.95 \text{ g/cm}^3$ ) dimensional change, such as presented in Figure 4 and Figure 5, are not available beyond a level of  $10.0 \times 10^{21} \text{ n/cm}^2$ .

For graphite with a lower density ( $1.5 - 1.75 \text{ g/cm}^3$ , i.e. graphite reflector material) some experimental data does exist [13] up to  $30 \times 10^{21}$ . However, there is a large scatter of the data, which depend on the graphite production process (Bacon Anisotropy Factor, or BAF, poor and high oriented crystals), irradiation temperature, and (fast) neutron flux. For all experiments it has been observed that as a function of neutron fluence the graphite first shrinks at the beginning of the irradiation. In some cases the shrinkage turns to swelling afterwards in the direction perpendicular to the basal planes, but shrinkage continues, in general, in the direction parallel to them. However, for the latter a turnaround point at high fluence levels ( $> 5.0 \times 10^{21} \text{ n/cm}^2$ ) can also exist, where the shrinkage turns into swelling, depending on the conditions.

Based on this expected behavior and the available data up to a fluence level of  $\sim 10.0 \times 10^{21} \text{ n/cm}^2$  a correlation can be derived for fluence levels up to  $30.0 \times 10^{21} \text{ n/cm}^2$  by extrapolation. In reference [14] this has been done based on experimental data from reference [15]. In this case a correlation of the following form was chosen:

$$S(\Phi) = a\Phi x^2 + b\Phi + c \quad (8)$$

in which  $S$  is the dimensional change in percentage,  $\Phi$  is the fast fluence and  $a$ ,  $b$  and  $c$  are constants determined by fitting of existing experimental data. The following values were used in [14] for equation (8):  $a = 0.140$  and  $b = -1.324$  for the tangential direction and  $a = 0.181$  and  $b = -1.066$  for the radial direction. The constant  $c$  was chosen to be zero for both directions. The advantage of this correlation in comparison with higher order polynomials is that it gives a correct zero strain for  $\Phi=0$ . Furthermore, the formula predicts, although speculative, a ‘turnaround’ of the shrinkage to swelling. However, the correlation predicts a turnaround of the tangential dimensional change at about  $5.0 \times 10^{21}$ , which does not compare well with the experimental data that show a continuation of the shrinkage (Figure 4 and Figure 5) for fluence levels between  $4.0$  and  $8.0 \times 10^{21} \text{ n/cm}^2$ . Therefore a slightly modified approach has been chosen here.

The fluence domain was split up in two parts. For fluence levels higher than  $1.5 \times 10^{21} \text{ n/cm}^2$  a second order polynomial has been chosen which allowed for a nonzero constant  $c$ , while for the low fluence levels ( $0 - 1.5 \times 10^{21} \text{ n/cm}^2$ )  $c = 0$ . The latter polynomial is fitted in such a way that a smooth function exists for the entire fluence domain. This is achieved by demanding that both the dimensional change as well as the dimensional change rate of both correlations are equal at  $1.5 \times 10^{21} \text{ n/cm}^2$ .

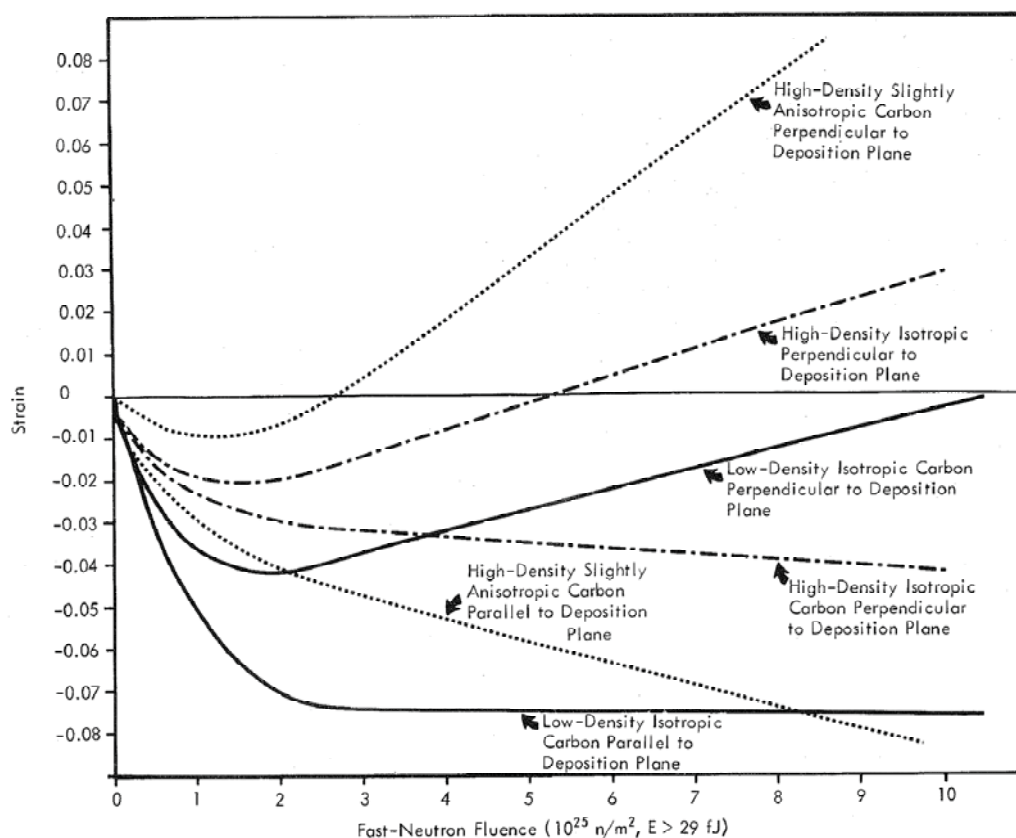


Figure 5. Dimensional change of PyC as a function of the fast ( $>E_c = 0.18 \text{ MeV}$ ) fluence for the radial and tangential directions for high density (isotropic and slightly anisotropic) and low density graphite, [16].

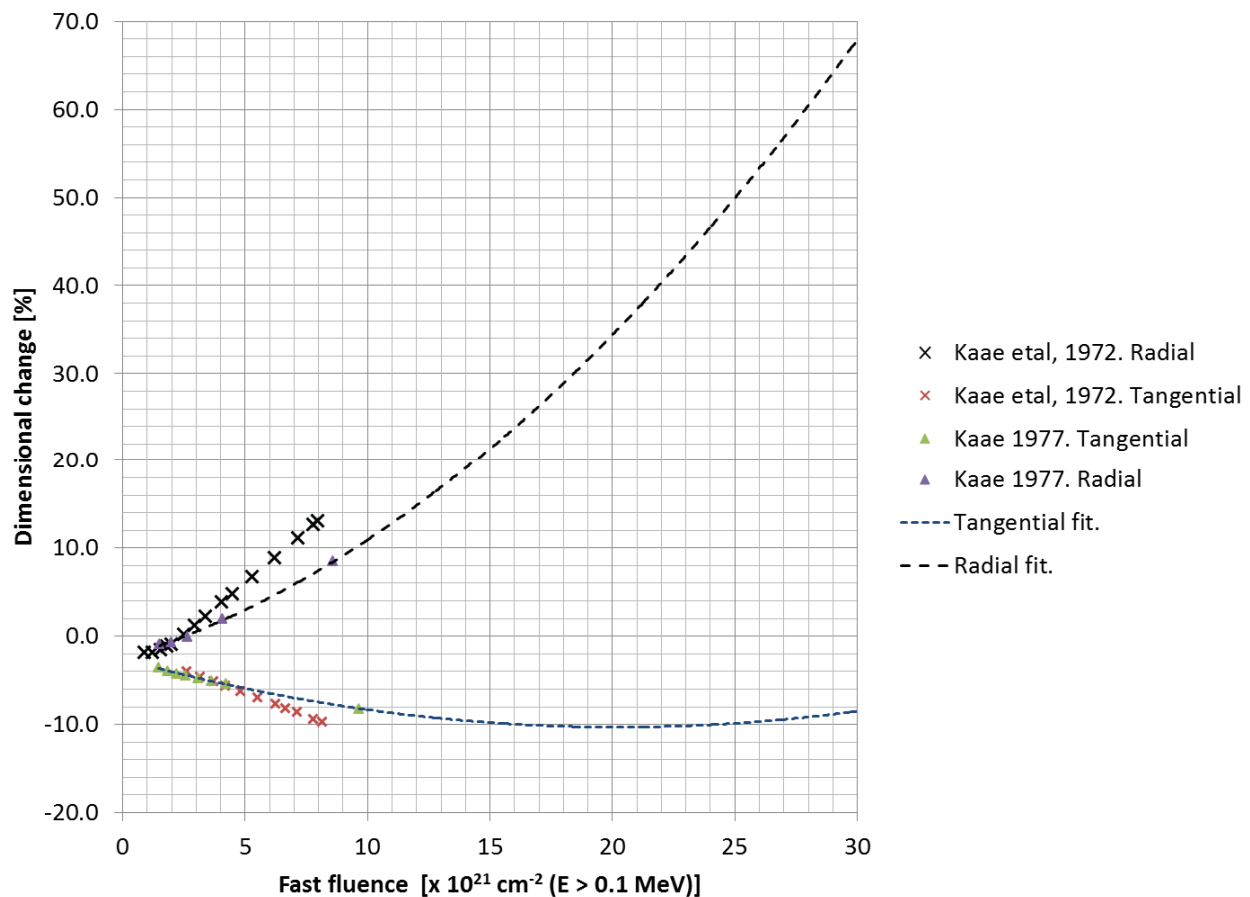


Figure 6. Dimensional change of PyC as a function of the fast (0.18 MeV) fluence for the radial and tangential directions for high density (slightly anisotropic) graphite [16] (denoted with ‘Kaae, 1977’) and its extrapolated values at high neutron fluence levels. Data from reference [12] has also been shown (Kaae et. al., 1972).

In Figure 6 the data of reference [16] is shown together with the second order polynomial curve fits for both directions including the results for fluence levels up to  $30.0 \times 10^{21} \text{ n/cm}^2$ . Data from reference [12] has also been shown for comparison. The constants for the radial and tangential direction of the fitted curves are, respectively:  $a = 5.044 \times 10^{-2}$ ,  $b = 8.335 \times 10^{-1}$ ,  $c = -2.430$  and  $a = 1.896 \times 10^{-2}$ ,  $b = -7.666 \times 10^{-1}$ ,  $c = -2.559$ . Figure 7 shows the fitted curves for the low fluence range ( $< 1.5 \times 10^{21} \text{ n/cm}^2$ ). The constants for the radial and tangential direction for these curves are, respectively:  $a = 1.130$ ,  $b = -2.407$ ,  $c = 0$  and  $a = 1.156$ ,  $b = -4.179$ ,  $c = 0$ .

It can be seen that the combined fits give a smooth function for the entire domain and correspond well with the experimental for both low and high fluence levels. It is noted here that the extrapolation of the data is far beyond the existing data and that the proposed function remains speculative, which should be substantiated with future experimental data.

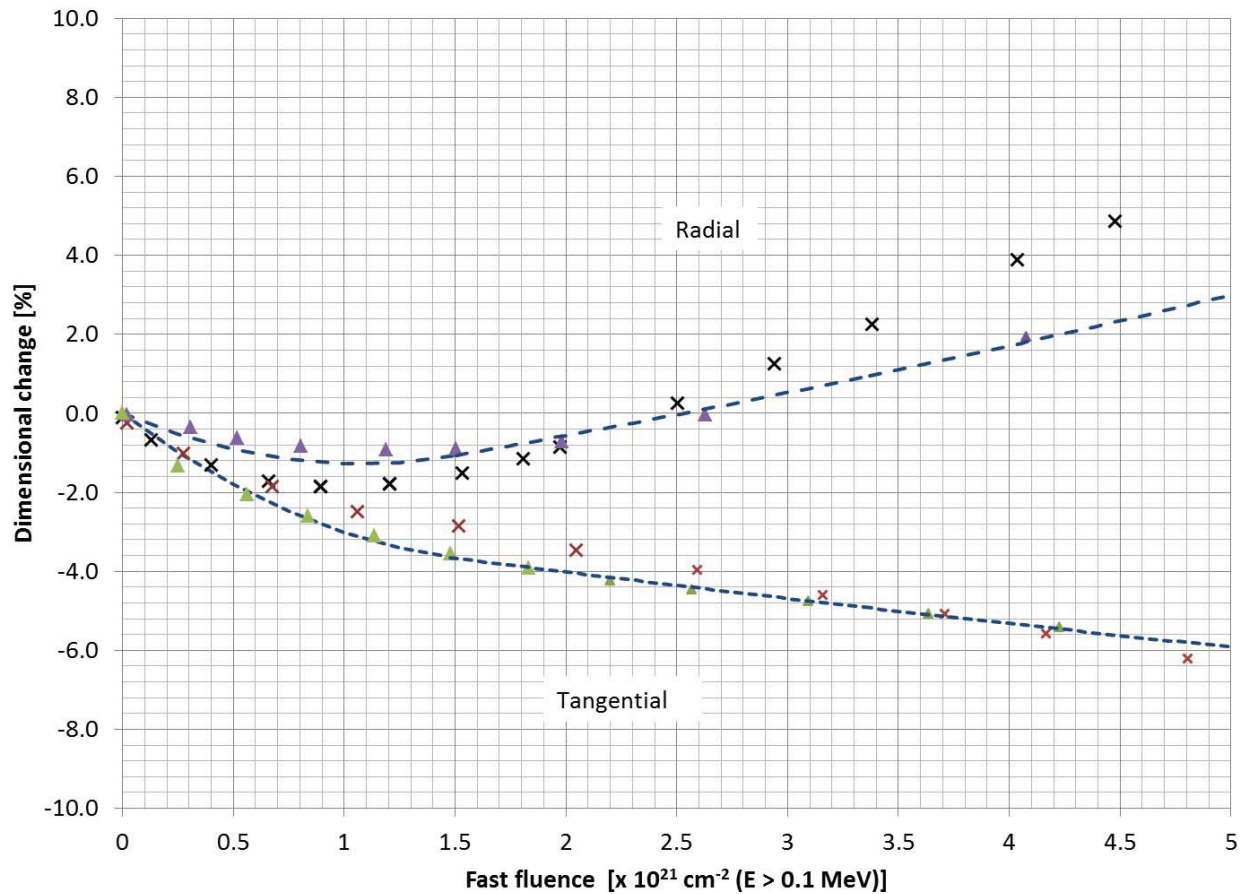


Figure 7. Dimensional change of PyC as a function of the fast (0.18 MeV) fluence for the radial and tangential directions for high density (slightly anisotropic) graphite [16] (denoted with 'Kaae, 1977') and its extrapolated values at high neutron fluence levels. Data from reference [12] has also been shown (Kaae et. Al., 1972).



## 4. DESCRIPTION OF THE PASTA CODE

The PASTA code [3,17] describes the mechanical behavior of TRISO particles during irradiation and aims at calculating the coating stresses and the corresponding failure probabilities. Typically, TRISO particles have a uranium/plutonium-oxide fuel kernel of several hundred micron in diameter at their very center. Adjacent to the kernel is a ~100  $\mu\text{m}$  thick porous carbon buffer, which is coated with an inner pyrolytic carbon (IPyC) layer, a silicon carbide (SiC) layer, and an outer pyrolytic carbon (OPyC) layer. These layers are typically in the range of 25-40 micron in thickness each. The coatings provide the primary containment of the fission products that are generated within the fuel kernel.

PASTA embodies a one-dimensional analytical and multi-layer model that takes into account the visco-elastic behavior of the coating layers and the surrounding matrix material (typically graphite or SiC) during irradiation. The main source of stress in all layers is due to the pressure build-up from the gaseous fission products in the buffer layer resulting in a radial stress on the IPyC. Moreover, the Pyrocarbon (IPyC and OPyC) layers exhibit radiation-induced dimensional changes and creep (in the radial and tangential directions). Finally, the model allows thermal expansion of all layers. PASTA solves the general stress strain equations, which include the aforementioned effects, and are as follows for the radial and tangential direction of a spherical layer, [3]:

$$\frac{\partial \varepsilon_r}{\partial t} = \frac{1}{E} \left[ \frac{\partial \sigma_r}{\partial t} - 2\mu \frac{\partial \sigma_t}{\partial t} \right] + c[\sigma_r - 2\nu\sigma_t] + \alpha_r \dot{T} + \dot{S}_r \quad (9)$$

$$\frac{\partial \varepsilon_t}{\partial t} = \frac{1}{E} \left[ (1 - \mu) \frac{\partial \sigma_t}{\partial t} - \mu \frac{\partial \sigma_r}{\partial t} \right] + c[(1 - \nu)\sigma_t - \nu\sigma_r] + \alpha_t \dot{T} + \dot{S}_t \quad (10)$$

The mechanical failure probability ( $\Psi$ ) of the coated particle is determined from the magnitude of the (tensile) stress in the SiC layer, which is the main load-bearer, according to the following Weibull distribution:

$$\Psi = 1 - \exp \left( -\ln(2) \left( \frac{\sigma_t}{\sigma_{med}} \right)^m \right) \quad (11)$$

in which  $\sigma_t$  is the tangential (tensile) stress in the SiC layer,  $\sigma_{med}$  the median (characteristic) strength of the SiC and  $m$  is the Weibull modulus of the SiC strength. These latter two parameters are taken to be  $\sigma_{med} = 340$  MPa and  $m = 5$ , [11].

The internal pressure in the coated particle results from gaseous fission products (Xe and Kr) that accumulate in the kernel and diffuse to the buffer layer during irradiation. The contribution of He to the internal pressure, by production via alpha decay, can also be taken into account if required. The buildup of gaseous fission products in the buffer can be calculated both analytically and numerically by solving the time-dependent fission product diffusion equation:

$$\frac{\partial C}{\partial t} = \frac{D(T)}{r^2} \left[ \frac{\partial}{\partial t} \left( r^2 \frac{\partial C}{\partial r} \right) \right] + \beta \quad (12)$$

in which  $\beta$  is the production rate of fission products and  $D(T)[\text{s}^{-1}\text{m}^2]$  is the temperature dependent diffusion coefficient.

In the PASTA code both a numerical method using a finite difference scheme and a fast analytical method for the calculation of the fractional release of fission products from the kernel to the buffer can be used.



The source term  $\beta$  is largely determined by production of the gaseous fission products Xe and Kr. Besides direct formation of gaseous fission products, formation of CO gas is possible by a reaction of the free oxygen present in the fuel kernel with the carbon in the buffer layer (in the case that there is no oxygen to prevent this).

The resulting pressure  $p$  (from both fission products and CO accumulation) on the IPyC layer is calculated as a function of the kernel temperature  $T$  and the buffer volume with the Redlich Kwong equation of state, [18]:

$$\text{-----} \tag{13}$$

in which  $R$ , is the universal gas constant and the constants  $a$  and  $b$  depend on the species. The ideal gas law is not used here, because it under predicts the pressure significantly.

As input parameters the code requires, the burnup level, fast fluence level, temperature (kernel and coating layers) and/or power as a function of the fuel residence time. Coupling of the PASTA code with detailed neutronics and thermal-hydraulics has been established for pebble-bed reactor modeling using the PEBBED code [19].

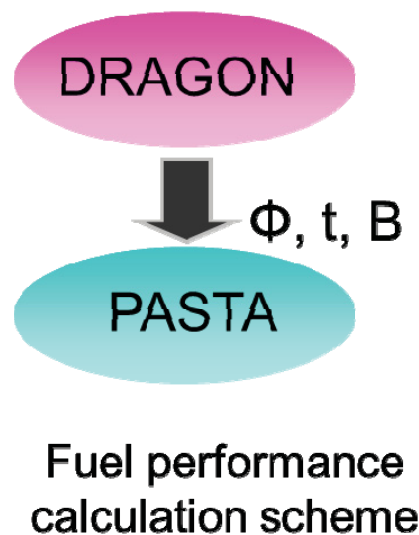


Figure 8. Overview of the DRAGON-PASTA calculation procedure for fuel performance analysis.

The code is also capable of performing simplified thermal calculations. The amount of fission gas generated can also be estimated by the code from the burnup level, in case it is not directly supplied by a neutronics code. The latter two simplifications have been adopted for the study presented in this report, in which only the burnup level, residence time, and fluence level were supplied by the DRAGON code (Figure 8).

The contribution of He to the fission gas pressure by the production of alpha decay is not taken into account in the current analysis. This contribution is expected to be an order of magnitude smaller than that of Xe and Kr combined.

## **5. DESCRIPTION OF THE NEUTRONIC ANALYSIS USING THE DRAGON CODE**

Neutronic calculations were performed using DRAGON-4, an open-source lattice transport code developed and maintained by École Polytechnique de Montréal [5]. This code contains multiple solution methods and allows for flexible calculation routes and data manipulation. The code also allows for treatment of the double-heterogeneity of the TRISO particles in the fuel directly using the method developed by Hébert [20]. Collision probability calculations were performed using a cross section library generated from ENDF/B-VII and cast in the SHEM-281 energy group structure [21].

In LWR analysis, calculations on a single unit cell can be informative with regard to the performance of a certain fuel in the whole core. Ultimately under investigation is how much TRU-only FCM fuel can be used in a LWR core. Therefore, the analysis must investigate how pins of this fuel type would affect the neutronic performance of an LWR were they used in conjunction with uranium fuel in, for example, heterogeneous assemblies. As a first step, the TRU-only FCM fuel is analyzed as a single unit cell as though it is the only fuel type present in the core. The results are interpreted with the knowledge that if the TRU-only pin is used in conjunction with  $\text{UO}_2$  pins or assemblies, the overall behavior would be expected to be the composite result of the effects of the TRU-only FCM unit cells and the  $\text{UO}_2$  unit cells.

A detailed description regarding the neutronic analysis of FCM with the DRAGON code can be found in reference [22].

## 6. STRESS ANALYSIS AND FUEL PERFORMANCE OF FCM FUEL

The performance of the coated particle fuel has been analyzed with the updated PASTA stress analysis cod. The boundary conditions, based on thermal calculation of Section 2.2 and neutronic assessment with the DRAGON code [5], assumed for the analysis of the fuel during normal operation are presented in Table 3. The material properties of the particle coating are given in Table 4.

**Table 3. Conditions of the FCM fuel during normal operation.**

Parameter	Value
Particle temperature	900 K
Final burnup	706 MWd/kg
Final fast fluence level	$17.8 \times 10^{21} \text{ cm}^{-2} (E > 0.1 \text{ MeV})$

**Table 4. Coating material properties taken from [11], [15], [16].**

Parameter	Value
Young's modulus of elasticity of PyC	$3.96 \times 10^4 \text{ MPa}$
Young's modulus of elasticity of SiC	$4.0 \times 10^5 \text{ MPa}$
Poisson ratio of elasticity of PyC	0.33
Poisson ratio of elasticity of SiC	0.13
Creep coefficient (radiation) of PyC	$4.1 \times 10^{-29} (\text{MPa}\cdot\text{n}/\text{cm}^2[E > 0.1 \text{ MeV}])^{-1}$
Creep coefficient (radiation) of SiC	$0. (\text{MPa}\cdot\text{n}/\text{cm}^2[E > 0.1 \text{ MeV}])^{-1}$
Poisson ratio of (radiation) creep PyC	0.4
Dimensional change PyC	See correlation Section 3.3

### 6.1 PERFORMANCE OF THE REFERENCE DESIGN UNDER NORMAL OPERATING CONDITIONS

In Figure 9 and Figure 10 the pressure in the buffer layer and the resulting stresses in the coating layers are shown for the fuel particle that has exactly the reference dimensions specified in the design.

The amount of fission gas release (FGR) from the fuel kernel to surrounding carbon buffer layer is not known for the specific fuel type (and conditions). Therefore a bounding value of 100 % FGR was assumed first for the calculations.

At the final burnup of 706 MWd/kg and 100 % FGR an internal pressure of 46 MPa and the maximum stress in the SiC layer of 224 MPa was calculated (Figure 11 for stress and pressure evolution). The latter stress level results in a failure probability of the SiC layer of  $8.2 \times 10^{-2}$  (Figure 12 for evolution).

In a second step the FGR fraction was varied between 10 - 100%. The results are shown in Figure 13 and Figure 14. One can see that the failure probability can drop orders of magnitude with reducing FGR fraction. Typical TRISO (UO<sub>2</sub>) fuel for HTRs can reach high release fraction of 70 % for T=1523K and 11% FIMA burnup, while the release can be an order of magnitude lower at a 200 K lower fuel temperature [23]. Inert Matrix Fuel (IMF), similar to FCM fuel, uses a matrix material (often a ceramic-ceramic or ceramic-metallic mixture with one phase being Zr or ZrO<sub>2</sub>) in combination with TRU fuel. According to experiments this fuel type has a FGR fraction between 25 % and 40 % for a burnup level of

about 575 MWd/kg iHM at a temperature range of 1200 - 1350 °C, [24]. In comparison, FCM fuel has a higher target burnup of ~700 MWd/kg, but will experience lower temperatures < 650 °C. Therefore, an estimated guess of the FGR based on the IMF data would be in the order of 50 %. For this FGR fraction the failure probability is estimated at  $\sim 1 \times 10^{-3}$  for the reference particle.

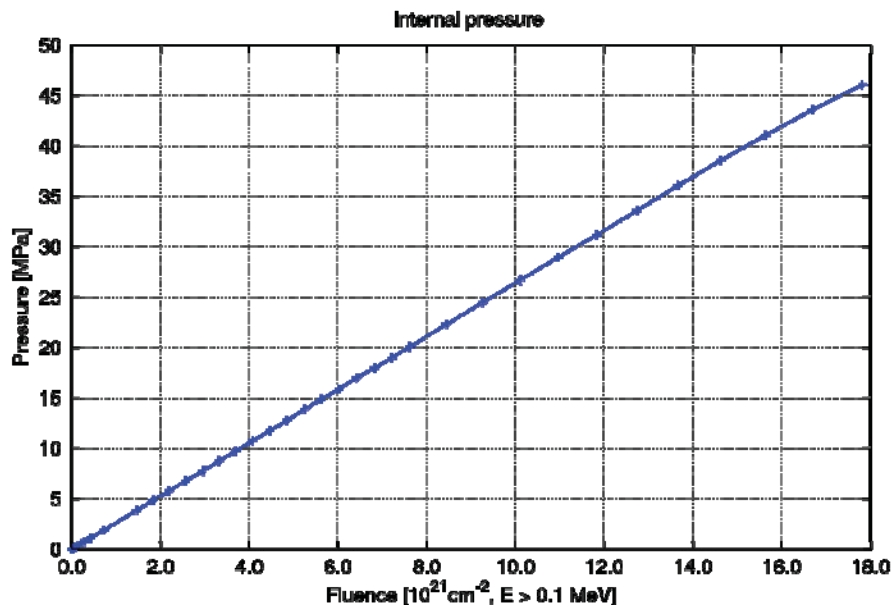


Figure 9. Pressure in the buffer layer of the coated from Xe and Kr release from the kernel.

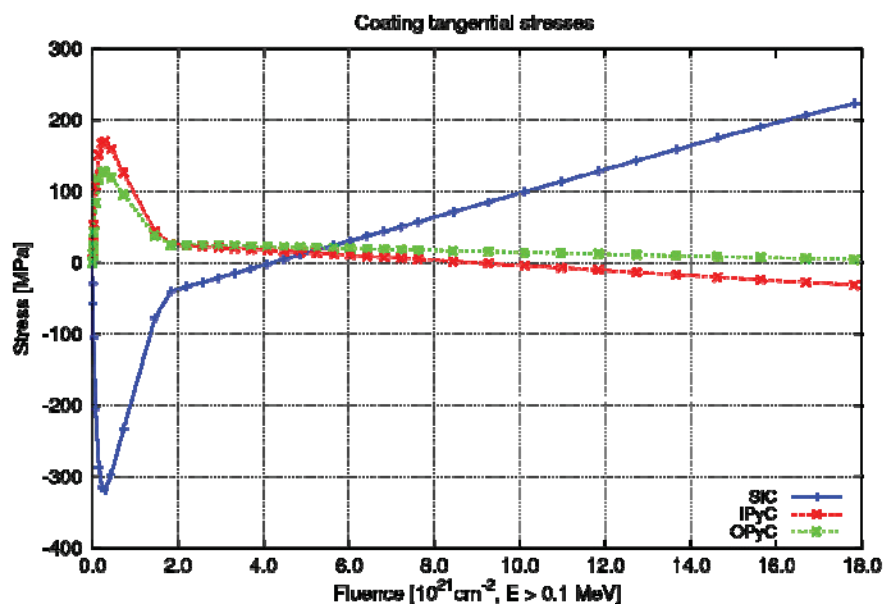


Figure 10. Tangential stresses in the coating layers during irradiation of the particle (with reference dimensions).

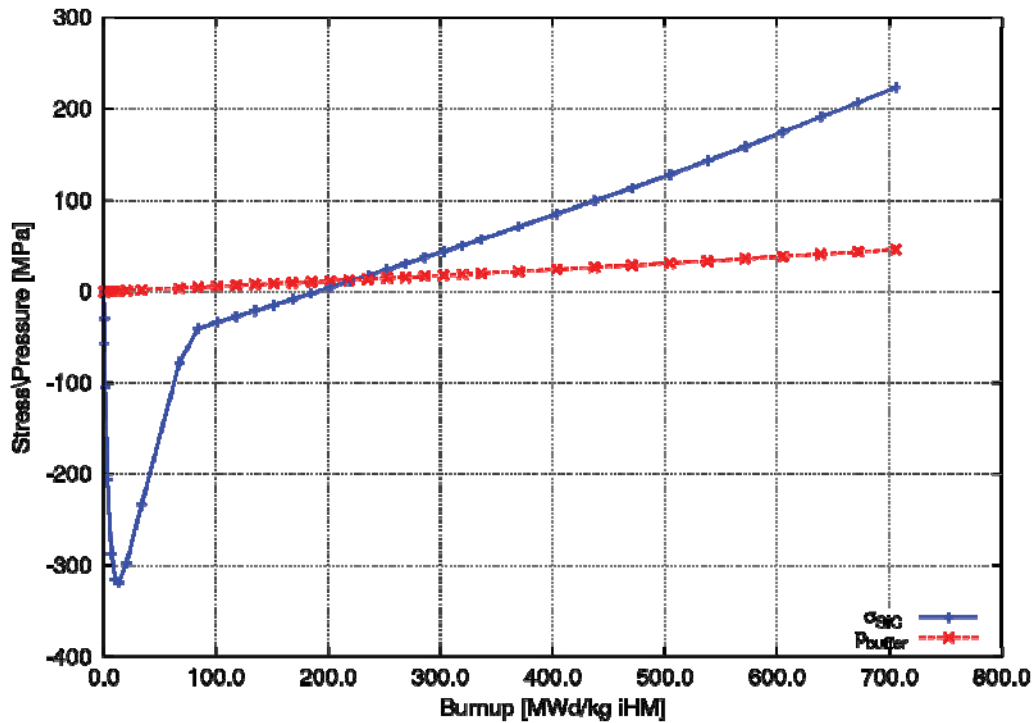


Figure 11. Tangential stress in the SiC layer and the pressure in the carbon buffer layer as a function of the burnup for the particle with the reference coating dimensions.

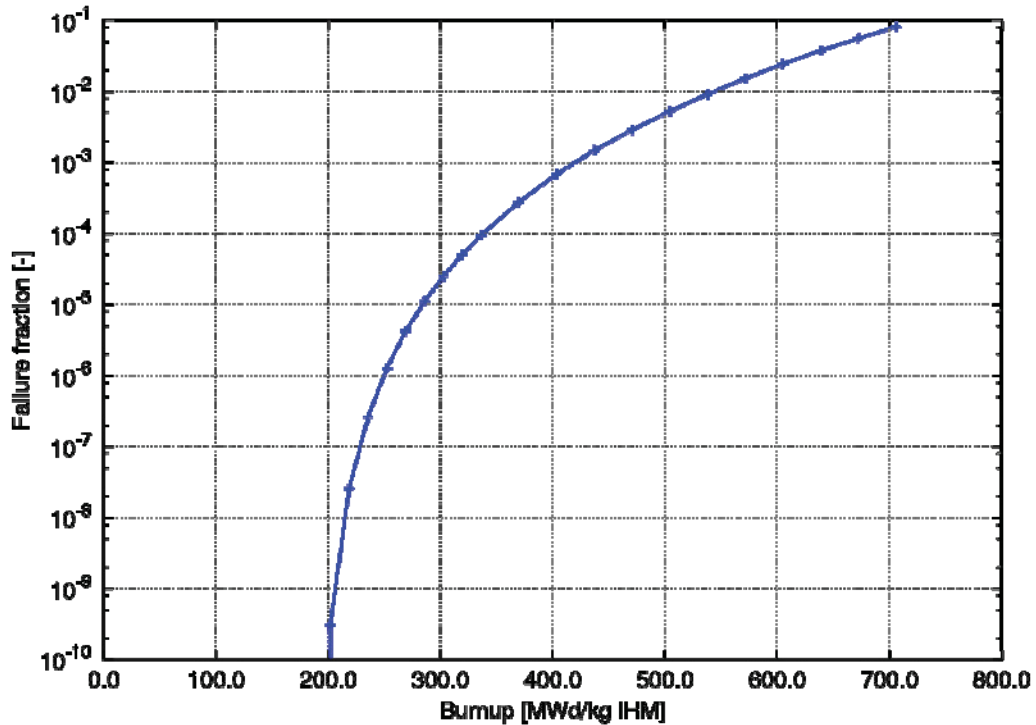


Figure 12. Failure probability as a function of the burnup for the particle with the reference coating dimensions.

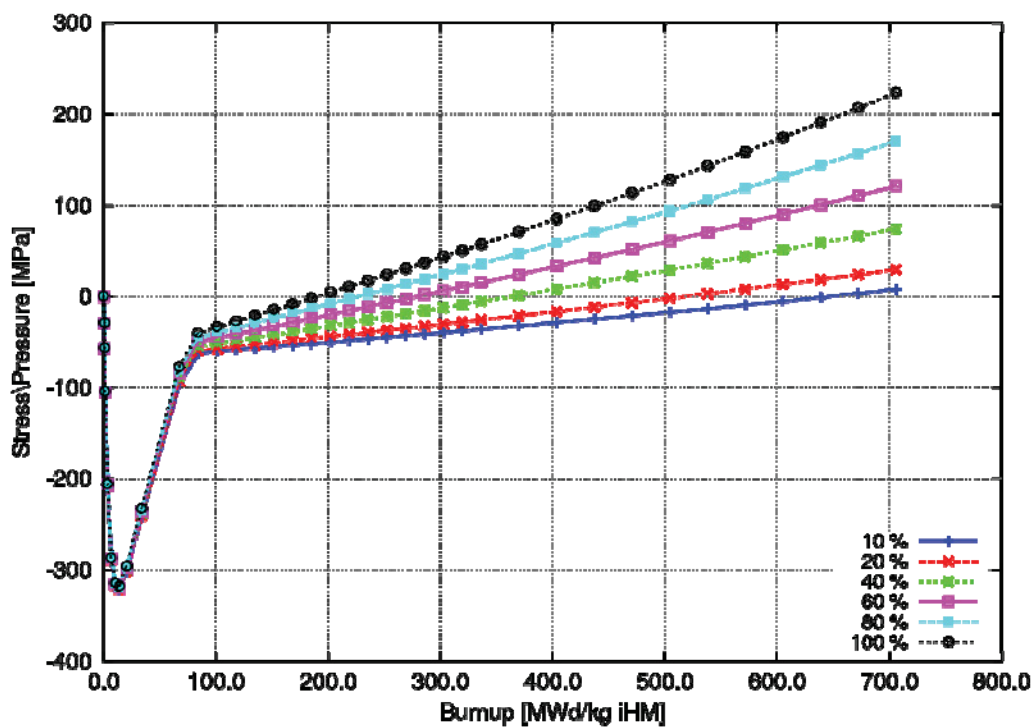


Figure 13. Tangential stress in the SiC layer as a function of the burnup for the particle with the reference coating dimensions with the percentage of fission gas release as a parameter.

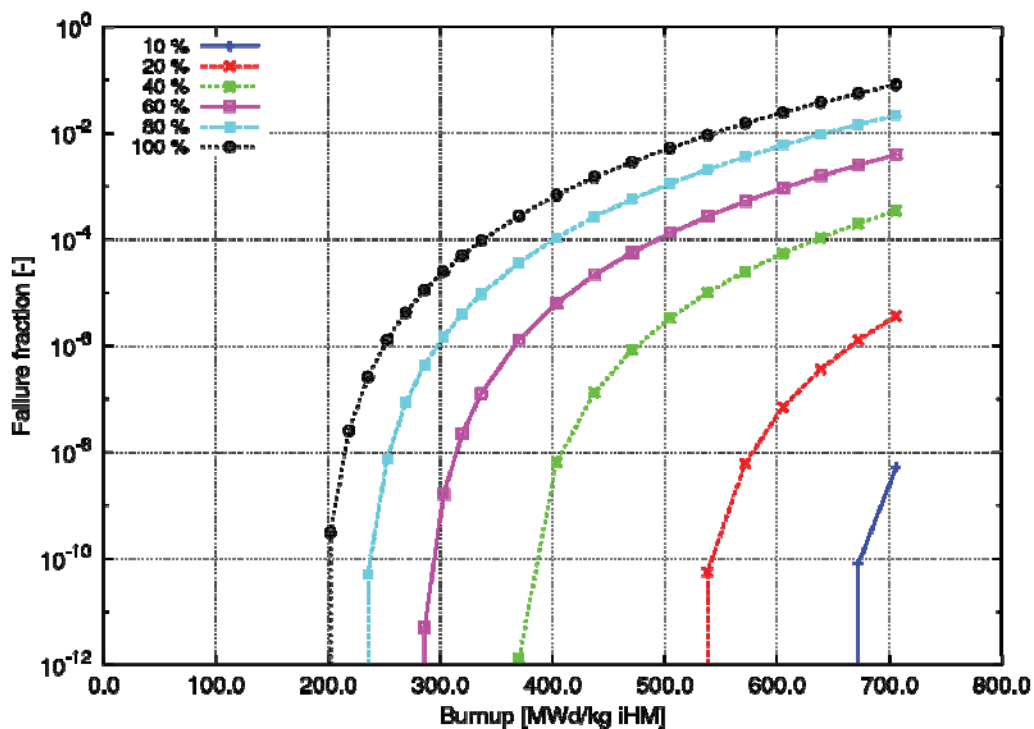


Figure 14. Failure probability as a function of the burnup for the particle with the reference coating dimensions with the fission gas release fraction as a parameter.

In the calculation results, shown in the figures above, it was assumed that the particles have the exact coating dimensions given in Table 1. In reality, as a result of the fabrication process, the thickness of the coating layers slightly varies for a batch of coated particles. The impact of the variations of the buffer layer and the SiC layer on the failure probability for a batch of particles has been estimated. It was assumed that the distribution of the thickness of both these layers for a batch can be described with a normal distribution with a standard deviation of 5  $\mu\text{m}$ . The estimated failure probability for a batch of particles was found to be  $1.1 \times 10^{-1}$ , assuming 100 % FGR. For a FGR fraction of 50 % the predicted failure probability drops to  $2.0 \times 10^{-3}$ .

## 6.2 IMPACT OF THE KERNEL SIZE ON THE FUEL PERFORMANCE

From a neutronics viewpoint it is advantageous to use a larger kernel size than the 350  $\mu\text{m}$  reference in order to load more heavy metal into the fuel rod. With increasing kernel radius and a fixed buffer size, the kernel volume per buffer volume increases according to the following equation:

$$\frac{V_{kern}}{V_{buf}} = \frac{R_{kern}^3}{(R_{kern} + t_{buf})^3 - R_{kern}^3} \quad (14)$$

The buffer pressure is linearly dependent of this volume ratio:

$$p = \frac{V_{kern} \psi \cdot RT}{V_{buf}} \quad (15)$$

Assuming a thin shell model the tangential stress in the SiC layer can be calculated from the pressure and the SiC layer thickness ( $t_{SiC}$ ) as follows:

$$\sigma_{t,SiC} = \frac{p \cdot (R_{kern} + t_{buf})}{2t_{SiC}} \quad (16)$$

Combining the above equations gives a correlation for the SiC stress as a function of the kernel size. The resulting effect on the coating stress can be described in a simplified way by adopting a thin-shell model for the stress analysis (see equations below).

$$\sigma_{t,SiC} = f \frac{(R_{kern} + t_{buf})R_{kern}^3}{(R_{kern} + t_{buf})^3 - R_{kern}^3} \quad (17)$$

where  $V$  is the volume,  $t$  is the thickness of the layer,  $R_{kern}$  and  $R_{buf}$  are the kernel and buffer radii,  $p$  is the pressure in the buffer,  $\psi$  is the fission gas release fraction  $\sigma_{t,SiC}$  is the tangential stress in the SiC layer,  $R$  is the universal gas constant,  $T$  is the temperature. It can be seen that for this model the stress level induced by the buffer pressure increases by a factor of three when the kernel diameter is increased from 350 to 600  $\mu\text{m}$ .

The PASTA code has also been used to investigate the impact of the kernel size on the SiC stress. The code performs a more detailed analysis as compared to equation (17), assuming a thick shell model and taking into account the effect of radiation induced dimensional change and creep of the PyC layers. The results can be seen in Figure 16. It can be seen that the impact on the stress is higher than predicted by equation (17) and that the stress levels reached are relatively high compared to the SiC characteristic strength (340 MPa). Therefore the kernel diameter cannot be increased without modifying other particle design parameters (such as the the buffer volume).

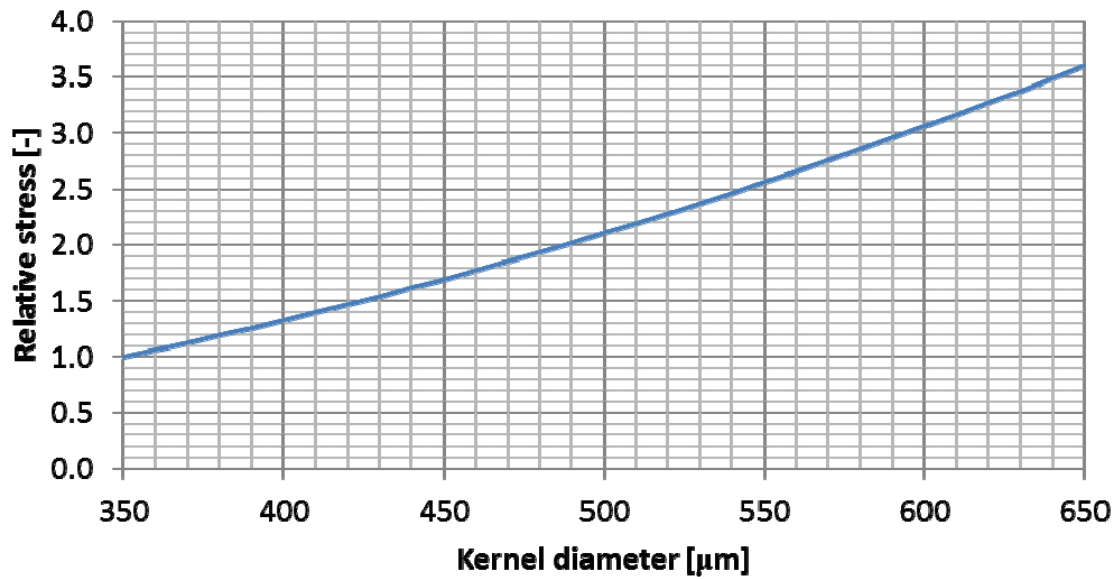


Figure 15. Impact of the kernel size on the relative stress in the SiC layer assuming a thin-shell stress model without creep and dimensional change.

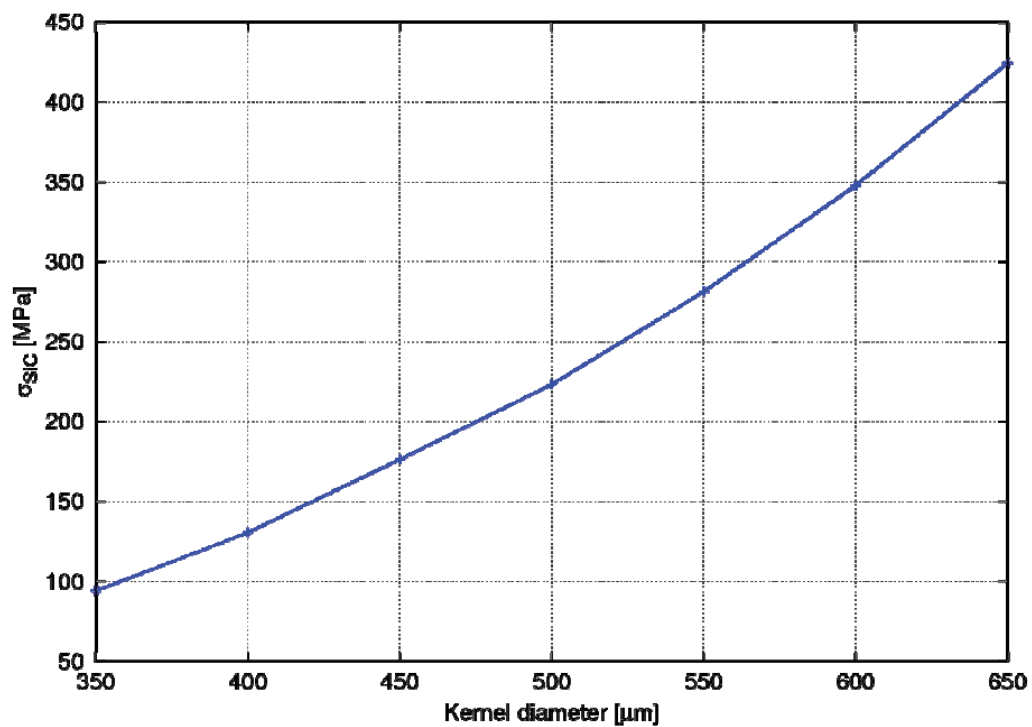


Figure 16. Tangential stress in the SiC layer as a function of the kernel diameter calculated with the PASTA code.



### 6.3 IMPACT OF THE SiC-MATRIX ON THE PARTICLE PERFORMANCE

In the analyses thus far, the presence of the SiC-matrix in which the coated particles are embedded has not been taken into account in the stress analysis. The SiC-matrix material is a stiff material, similar to the SiC coating layer. The displacement of the outer surface of the OPyC layer by (indirect) radiation effects will therefore induce stresses in the coating layers and the SiC-matrix itself.

The impact of the presence of the SiC-matrix on the stress state of the coatings has been investigated by adopting a 4-layer stress model, which includes the SiC-matrix as an additional layer next to the IPyC, SiC and OPyC layers (see Figure 17). In practice, a given particle is surrounded by both the SiC-matrix and its neighboring particle. Therefore, the addition of this layer with a fixed thickness is a rough simplification of the reality. The distance between randomly distributed particles in a matrix material, which is indicative for this layer thickness, has been calculated in reference [25] for typical loadings of 5000, 15,000 and 35,000 particles per pebble used in a High Temperature Reactor. It was shown that the following correlation gives a reasonable estimation for the cumulative distribution of the inter-particle distance ( $f_d$ ), when a ‘cut-off’ distance (equal to the particle diameter plus 180  $\mu\text{m}$  for high loadings) is used:

$$f_d = 1 - e^{(-4/3\pi\mu r_c^3)} \tag{18}$$

with  $\mu$  the particle density and  $r_c$  the center-to-center particle distance.

For the loading of 35,000 particles per pebble the above correlation predicts that the distance between the particle outer surfaces is about the 180  $\mu\text{m}$  cut-off or less for 95 % of the particles. The envisaged FCM fuel has a packing fraction of 44 % ( $\mu = 1070 \text{ cm}^{-3}$ ), which would be equivalent to a loading of 70,000 particles per pebble. As a result 99.9 % of the particles would have a neighbor at a surface-to-surface distance of 180  $\mu\text{m}$  or less. Using equation (18), one can estimate that 98 % of the particles have a neighbor at 50  $\mu\text{m}$  or less, and it can therefore be assumed that the average distance would be only several microns.

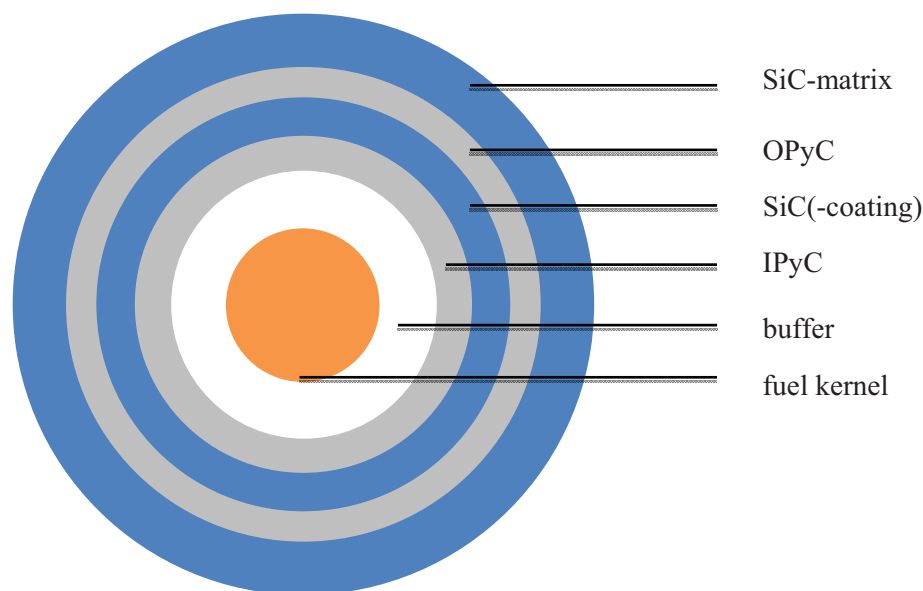


Figure 17. Schematic overview of the coating layers surrounding the FCM fuel kernel, which are embedded in the SiC-matrix.

The reference fuel has been analyzed, using a 4-layer stress model, with a SiC-matrix layer thickness of 1, 5, 10 and 20 micron. Furthermore, similar cases were analyzed, in which it was assumed that the OPyC was absent.

Table 5. Maximum tensile stress in the SiC layer for a particle surround by SiC-matrix material.

	SiC matrix layer thickness	Reference particle design	Design without OPyC
-	0 $\mu\text{m}$	224 MPa	236 MPa
a	1 $\mu\text{m}$	88 MPa	230 MPa
b	5 $\mu\text{m}$	163 MPa	207 MPa
c	10 $\mu\text{m}$	270 MPa	184 MPa
d	20 $\mu\text{m}$	404 MPa	151 MPa

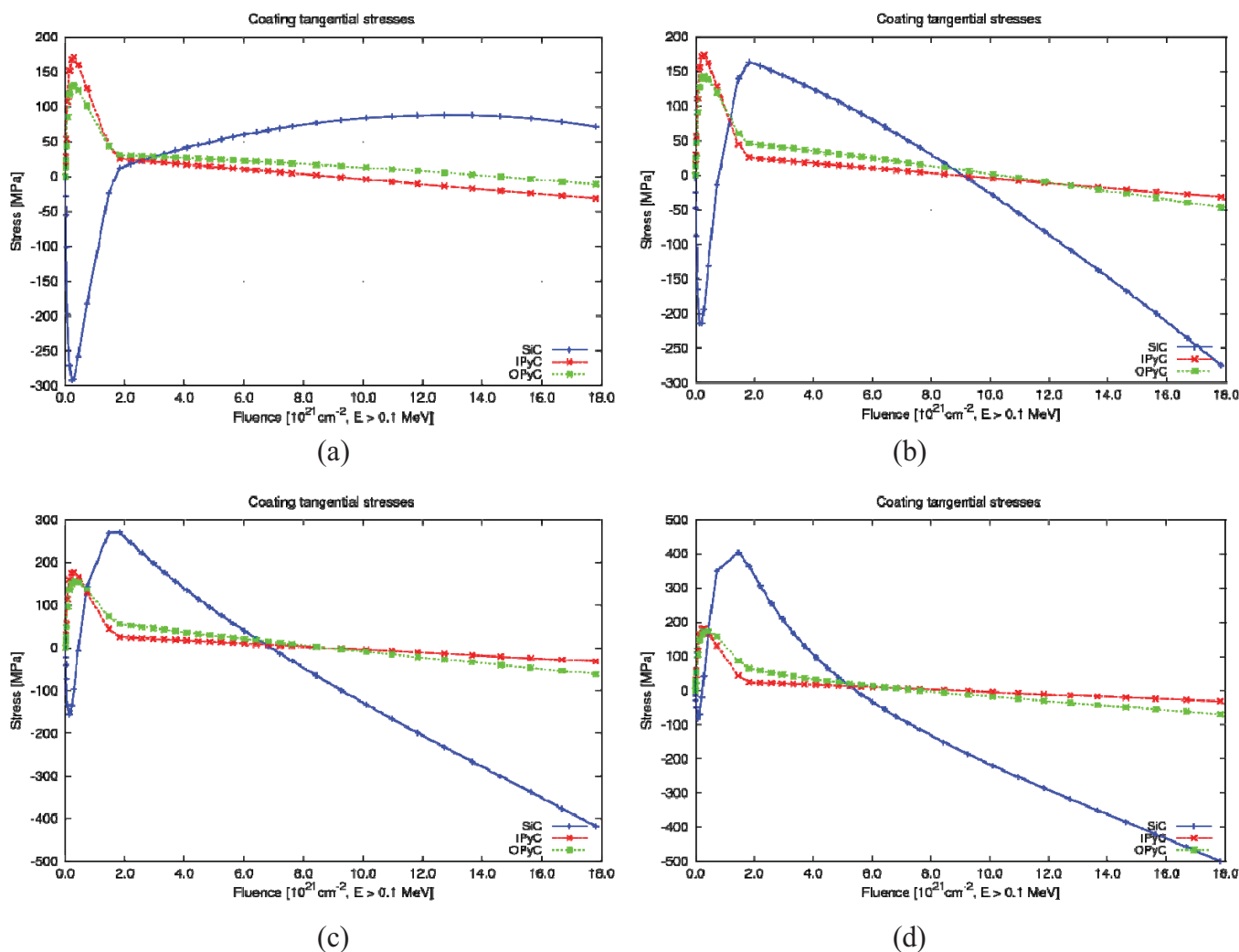


Figure 18. Coating stresses in the reference particle design as a function of the fast neutron fluence for the case that the particle is surrounded by SiC-matrix layer with a thickness of 1  $\mu\text{m}$  (a), 5  $\mu\text{m}$  (b), 10  $\mu\text{m}$  (c), or 20  $\mu\text{m}$  (d).

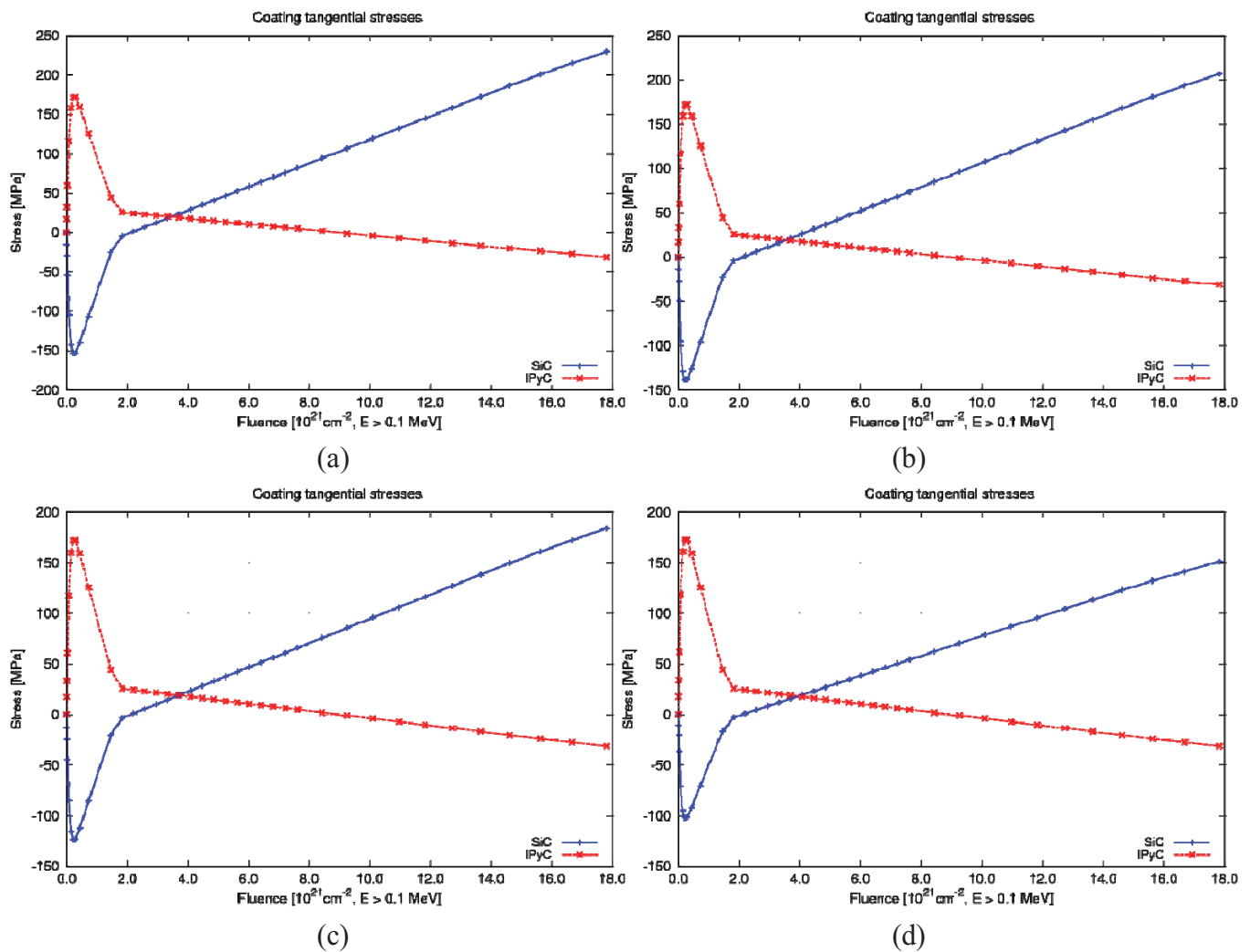


Figure 19. Coating stresses in coated particle design without an OPyC layer as a function of the fast neutron fluence for the case that the particle is surrounded by SiC-matrix layer with a thickness of 1  $\mu\text{m}$  (a), 5  $\mu\text{m}$  (b), 10  $\mu\text{m}$  (c), or 20  $\mu\text{m}$  (d).

The presence of the SiC-matrix reduces the movement of the outer surface of the OPyC. In the radial direction this layer shrinks first (below a level of  $1.0 \times 10^{21} \text{cm}^{-2}$ ) and then swells as a function of the neutron fluence. It can be seen from Figure 18 that with increased SiC-matrix thickness, and therefore increased immobility of the OPyC outer surface, the shrinkage at low fluence levels results in high tensile stress in the SiC-coating. Furthermore, the swelling of the OPyC at higher fluence levels results in a high SiC-coating compressive stress.

For the cases in which the OPyC layer is not included in the particle design, the stress evolution (Figure 19) follows a similar trend as the reference particle without SiC-matrix present (Figure 10). In this case the stresses in the coating layer are reduced by the presence of the SiC-matrix. In fact, with the OPyC absent, the SiC-matrix layer is located next to the SiC layer (Figure 17), which is now effectively increased in thickness.

It is noted that in the case that a given particle is surrounded by only a small layer of SiC-matrix it is likely to have one or several neighboring particles in its vicinity. Their presence would, similarly to the

presence of a thick SiC-matrix layer, reduce the potential displacement of the OPyC outer surface. Therefore, also in this case high (local) stresses could exist.

In the analyses above it was assumed that the outer surface of OPyC is connected to the inner surface of the SiC-matrix for the entire time (fluence) domain. If this interface would not be linked (by design), the shrinkage of the OPyC at low fluence levels would not lead to a high tensile SiC-coating stress at low fluence levels, since the OPyC outer surface can move freely in the inward direction. On the other hand, beyond a certain fluence level this particle would benefit from the continued swelling of the OPyC, which is limited by the presence of the SiC-matrix. Therefore, this swelling would result in a compressive stress in the SiC-coating layer.

## 7. OPTIMIZATION OF THE FCM COATED PARTICLE DESIGN

In the previous sections it was shown that the reference particle does not perform well for the targeted high burnup level of ( $\sim 700$  MWd/kg iHM). Furthermore, with regard to the neutronic performance of the fuel it is desirable to increase the TRU loading per pellet. It was shown in Section 6.2 that this cannot be achieved by increasing the kernel diameter, since this would lead to a high particle failure fraction.

As a first optimization step several design modifications have been investigated both regarding the neutronic performance, using the DRAGON code [5], as well as an analysis using the PASTA code. In a second step the most promising design is further optimized with regard to the fuel performance.

### 7.1 IMPACT OF DESIGN MODIFICATIONS ON PERFORMANCE

Table 6. Reference and modified particle designs and their TRU loading per pellet (deviations from the reference design are indicated in grey).

Case	Case Description	Kernel Diameter	Buffer Thick.	Coating Layer Thicknesses			Getter Volume	TRU Loading in pellet
				IPyC	SiC	OPyC		
1	Reference	500 $\mu\text{m}$	100 $\mu\text{m}$	35 $\mu\text{m}$	35 $\mu\text{m}$	40 $\mu\text{m}$	25 %	0.47 g/cm <sup>3</sup>
2	Larger kernel	600 $\mu\text{m}$	100 $\mu\text{m}$	35 $\mu\text{m}$	35 $\mu\text{m}$	40 $\mu\text{m}$	25 %	0.59 g/cm <sup>3</sup>
3	Large kernel, no getter	600 $\mu\text{m}$	100 $\mu\text{m}$	35 $\mu\text{m}$	35 $\mu\text{m}$	40 $\mu\text{m}$	0	0.78 g/cm <sup>3</sup>
4	Thin buffer	500 $\mu\text{m}$	75 $\mu\text{m}$	35 $\mu\text{m}$	35 $\mu\text{m}$	40 $\mu\text{m}$	25 %	0.54 g/cm <sup>3</sup>
5	Thin buffer, no getter	500 $\mu\text{m}$	75 $\mu\text{m}$	35 $\mu\text{m}$	35 $\mu\text{m}$	40 $\mu\text{m}$	0	0.71 g/cm <sup>3</sup>
6	Thinner buffer	500 $\mu\text{m}$	50 $\mu\text{m}$	35 $\mu\text{m}$	35 $\mu\text{m}$	40 $\mu\text{m}$	25 %	0.63 g/cm <sup>3</sup>
7	Thinner buffer, no getter	500 $\mu\text{m}$	50 $\mu\text{m}$	35 $\mu\text{m}$	35 $\mu\text{m}$	40 $\mu\text{m}$	0	0.84 g/cm <sup>3</sup>
8	No OPyC	500 $\mu\text{m}$	100 $\mu\text{m}$	35 $\mu\text{m}$	35 $\mu\text{m}$	0	25 %	0.58 g/cm <sup>3</sup>
9	No OPyC	500 $\mu\text{m}$	75 $\mu\text{m}$	35 $\mu\text{m}$	35 $\mu\text{m}$	0	25 %	0.69 g/cm <sup>3</sup>
10	No OPyC, thin SiC	500 $\mu\text{m}$	50 $\mu\text{m}$	35 $\mu\text{m}$	35 $\mu\text{m}$	0	25 %	0.83 g/cm <sup>3</sup>

Several modified particle designs have been investigated with the aim of increasing TRU loading per pellet (Table 6). In order to achieve this higher loading the following options have been investigated:

- Larger kernel diameter (case 2 and 3).
- Thinner buffer layer (cases 4 through 7 and cases 9, 10).
- Removal of the getter (case 3, 5, 7).

The resulting performance of the particles designs are given in Table 6. Figure 20 gives an overview of the particle failure fraction for the different cases at burnup levels of 500, 600 and 700 MWd/kg iHM. From the overview it can be seen that all modified designs perform worse than the reference design. Case 8 performs the best if only the modified cases are considered. None of the considered cases, which include the reference design, meet the design limit for the failure fraction of  $2.0 \times 10^{-5}$ , which is the typical performance level of coated particle fuel established during the German HTR research program in the past [26]. It is noted here that in the calculations a conservative value of 100 % FGR was assumed.

Table 7. Results of PASTA and DRAGON calculations for the reference and modified particle designs.

500 MWd/kg iHM								
	Burnup (MWd/kg iHM)	EFPD (days)	Flux ( $10^{14}$ cm <sup>-2</sup> s <sup>-1</sup> )	Fast Flux ( $10^{14}$ cm <sup>-2</sup> s <sup>-1</sup> )	Fast Fluence ( $10^{22}$ cm <sup>-2</sup> )	Int. Pressure (MPa)	SiC stress (MPa)	Failure Fraction
Nominal	504	700	4.00	1.98	1.10	31	128	$5.3 \times 10^{-3}$
Case2	504	900	3.90	2.00	1.41	41	216	$7.0 \times 10^{-2}$
Case3	497	1200	3.78	2.01	1.88	41	205	$5.4 \times 10^{-2}$
Case4	512	850	3.95	1.99	1.33	49	207	$5.7 \times 10^{-2}$
Case5	490	1100	3.76	1.99	1.71	65	296	0.29
Case6	500	1000	3.82	1.98	1.55	90	378	0.69
Case7	500	1350	3.73	2.00	2.10	139	616	1.00
Case8	512	950	4.15	2.15	1.59	32	160	$1.6 \times 10^{-2}$
Case9	511	1150	3.83	2.00	1.79	49	233	0.10
Case10	507	1400	3.75	2.00	2.17	92	413	0.84

600 MWd/kg iHM								
	Burnup (MWd/kg iHM)	EFPD (days)	Flux ( $10^{14}$ cm <sup>-2</sup> s <sup>-1</sup> )	Fast Flux ( $10^{14}$ cm <sup>-2</sup> s <sup>-1</sup> )	Fast Fluence ( $10^{22}$ cm <sup>-2</sup> )	Int. Pressure (MPa)	SiC stress (MPa)	Failure Fraction
Nominal	605	850	4.66	2.15	1.37	39	175	$2.5 \times 10^{-2}$
Case2	610	1100	4.55	2.17	1.77	51	291	0.27
Case3	596	1450	4.29	2.17	2.33	52	274	0.21
Case4	597	1000	4.46	2.13	1.60	59	267	0.19
Case5	597	1350	4.31	2.15	2.16	86	412	0.84
Case6	595	1200	4.33	2.12	1.91	119	518	0.99
Case7	607	1650	4.27	2.18	2.64	210	947	1.00
Case8	614	1150	4.78	2.33	1.98	39	206	$5.5 \times 10^{-2}$
Case9	596	1350	4.28	2.14	2.15	59	290	0.27
Case10	595	1650	4.17	2.14	2.62	118	541	0.99

700 MWd/kg iHM								
	Burnup (MWd/kg iHM)	EFPD (days)	Flux ( $10^{14}$ cm <sup>-2</sup> s <sup>-1</sup> )	Fast Flux ( $10^{14}$ cm <sup>-2</sup> s <sup>-1</sup> )	Fast Fluence ( $10^{22}$ cm <sup>-2</sup> )	Int. Pressure (MPa)	SiC stress (MPa)	Failure Fraction
Nominal	706	1000	6.07	2.45	1.67	46	224	$8.0 \times 10^{-2}$
Case2	716	1300	6.00	2.51	2.18	62	370	0.65
Case3	716	1750	5.65	2.53	2.94	71	390	0.75
Case4	711	1200	5.93	2.47	2.00	74	352	0.56
Case5	725	1650	5.90	2.56	2.77	129	637	1.00
Case6	714	1450	5.76	2.48	2.41	165	738	1.00
Case7	732	2000	5.78	2.58	3.36	417	1881	1.00
Case8	716	1350	6.17	2.67	2.42	47	253	0.15
Case9	724	1650	5.82	2.53	2.76	76	382	0.71
Case10	735	2050	5.77	2.58	3.44	174	803	1.00

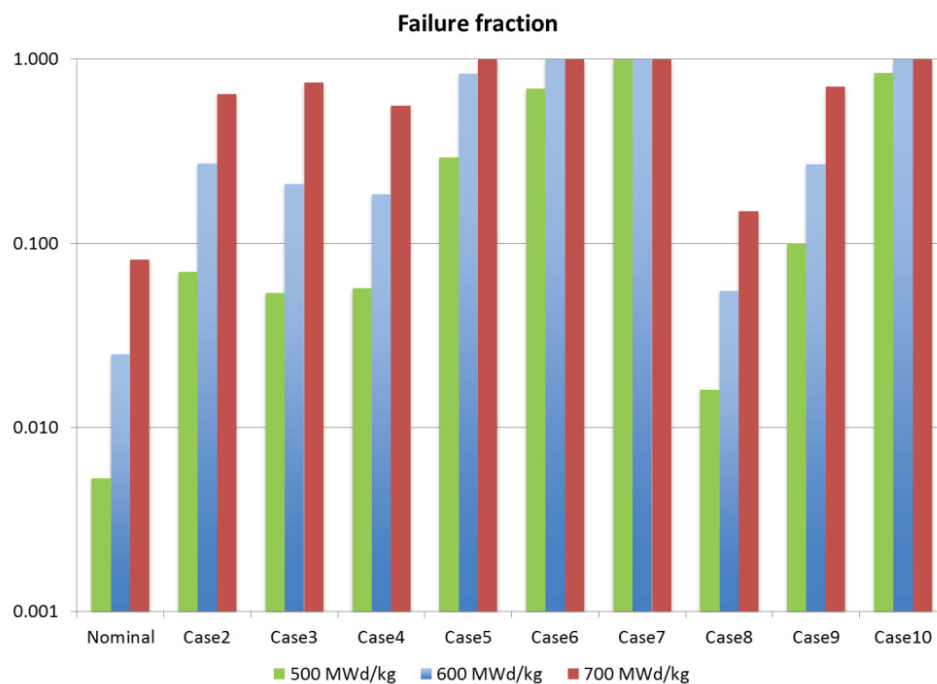


Figure 20. Failure probabilities of the various particle designs (presented in Table 6) at burnup levels of 500, 600 and 700 MWd/kg iHM.

## 7.2 OPTIMIZATION OF THE BUFFER AND OPyC THICKNESS

In order to improve the fuel performance of the particle an increase of the buffer volume is desirable. This would help to accommodate the fission gas, which is released from the fuel kernel during irradiation. An increase of the buffer while keeping the other coating thicknesses at a fixed value would however reduce the TRU loading per pellet. This is unacceptable with regard to the reactivity temperature coefficient. Therefore, the design is optimized with regard to the failure fraction, while keeping the particle outer radius at close to the reference value of 460  $\mu\text{m}$ . This corresponds to a TRU loading of 0.47  $\text{g}/\text{cm}^3$ .

In Section 6.3 it was shown that the presence of the OPyC layer in a particle, which is embedded in a SiC-matrix, is not always advantageous. Therefore, the buffer layer has been increased at the expense of the OPyC layer thickness. In the analysis it was assumed that the particle is surrounded by a 5  $\mu\text{m}$  thick SiC-matrix.

Table 8 shows the results of the analysis. It was found that the particles with an OPyC thickness of 10  $\mu\text{m}$  perform the best. Furthermore, the performance improves with increasing buffer thickness. This OPyC thickness combined with a buffer size of 120  $\mu\text{m}$  has been adopted for further calculations. If a larger buffer size would be chosen the TRU loading would be lower than that of the reference design.

Figure 22 shows the performance of the optimized particle in which the fraction of fission gas release was varied. It can be seen that the particle performs within the design limit of  $2.0 \times 10^{-5}$  for FGR fractions of 50 % and lower.

Table 8. Particle performance for several combinations of the buffer and OPyC layer thicknesses.

	SiC-matrix layer thickness	Buffer thickness	OPyC thickness	Particle radius	TRU loading	Maximum SiC-coating stress	Failure fraction
0	5 μm	100 μm	40 μm	460 μm	0.47 g/cm <sup>3</sup>	163 MPa	1.8 x 10 <sup>-2</sup>
1	5 μm	120 μm	40 μm	480 μm	0.41 g/cm <sup>3</sup>	154 MPa	1.3 x 10 <sup>-2</sup>
2	5 μm	140 μm	40 μm	500 μm	0.36 g/cm <sup>3</sup>	146 MPa	1.0 x 10 <sup>-2</sup>
3	5 μm	160 μm	40 μm	520 μm	0.32 g/cm <sup>3</sup>	139 MPa	7.9 x 10 <sup>-2</sup>
4	5 μm	120 μm	0 μm	440 μm	0.53 g/cm <sup>3</sup>	164 MPa	1.8 x 10 <sup>-2</sup>
5	5 μm	140 μm	0 μm	460 μm	0.47 g/cm <sup>3</sup>	135 MPa	6.9 x 10 <sup>-3</sup>
6	5 μm	160 μm	0 μm	480 μm	0.41 g/cm <sup>3</sup>	114 MPa	3.0 x 10 <sup>-3</sup>
7	5 μm	120 μm	10 μm	450 μm	0.50 g/cm <sup>3</sup>	65 MPa	1.9 x 10 <sup>-4</sup>
8	5 μm	140 μm	10 μm	470 μm	0.44 g/cm <sup>3</sup>	55 MPa	7.8 x 10 <sup>-5</sup>
9	5 μm	160 μm	10 μm	490 μm	0.39 g/cm <sup>3</sup>	47 MPa	3.6 x 10 <sup>-5</sup>
10	5 μm	120 μm	20 μm	460 μm	0.53 g/cm <sup>3</sup>	89 MPa	8.7 x 10 <sup>-4</sup>
11	5 μm	140 μm	20 μm	480 μm	0.47 g/cm <sup>3</sup>	82 MPa	5.7 x 10 <sup>-4</sup>
12	5 μm	160 μm	20 μm	500 μm	0.41 g/cm <sup>3</sup>	76 MPa	3.9 x 10 <sup>-4</sup>

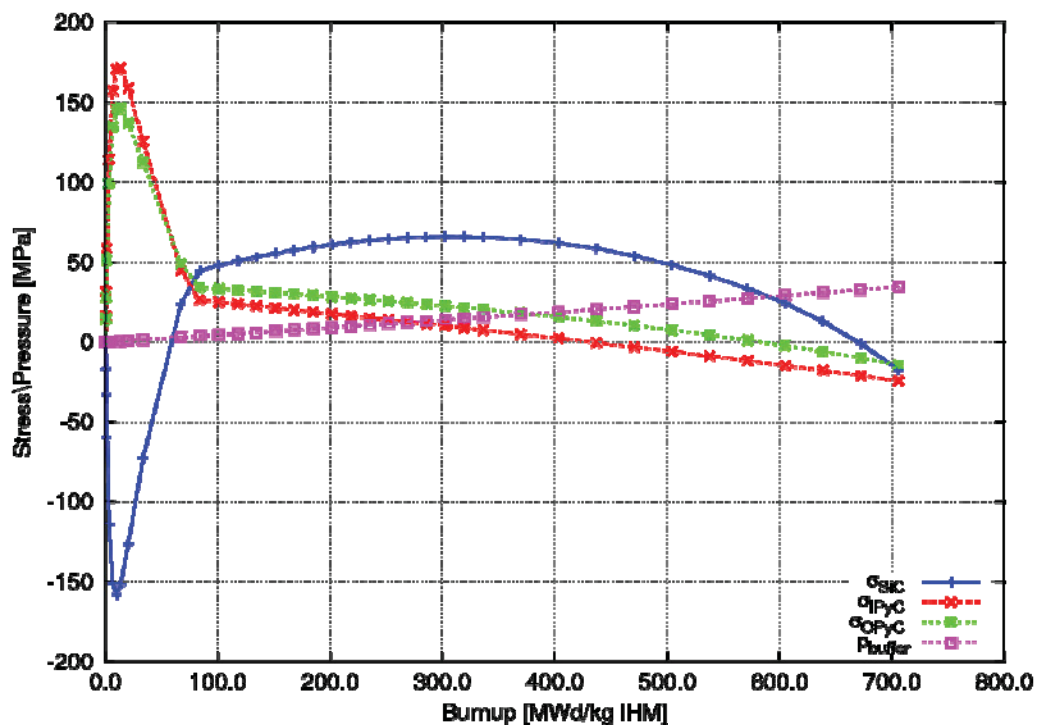


Figure 21. Tangential stresses in the coating layers and the buffer pressure as a function of the burnup for the particle with a buffer thickness of 120 micron and an OPyC thickness of 10 micron.



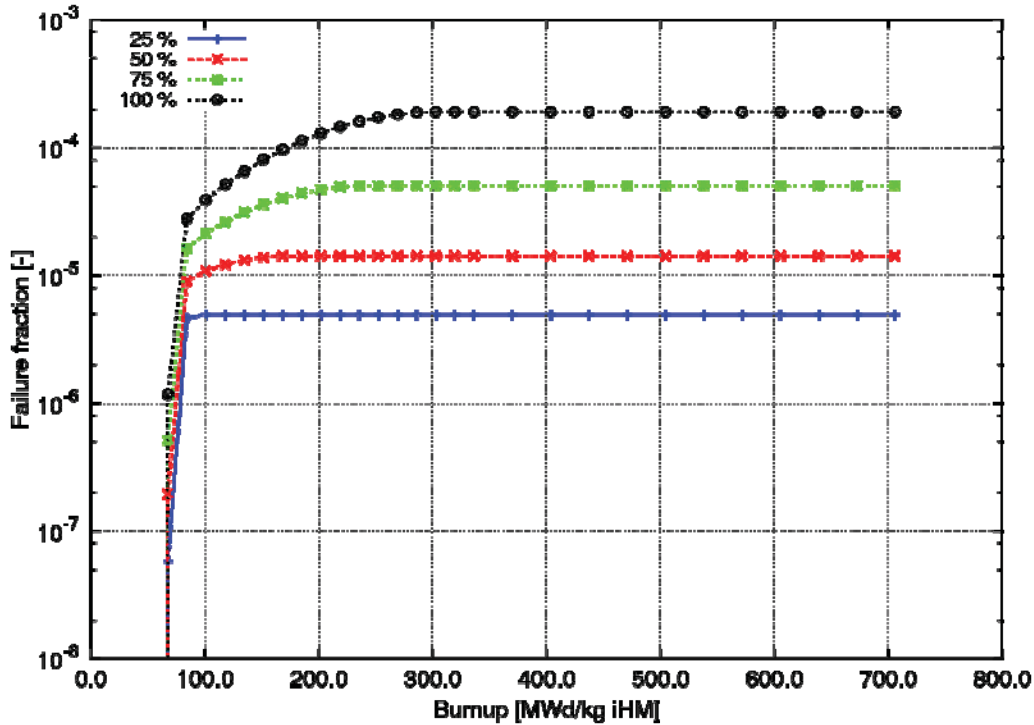


Figure 22. Failure probability as a function of the burnup for the particle with a buffer thickness of 120 micron and a OPyC thickness of 10 micron, with the fission gas release fraction as a parameter.

### 7.3 FUEL PERFORMANCE AT LOSS OF COOLANT ACCIDENT CONDITIONS

An analysis of the fuel performance during a Loss Of Coolant Accident (LOCA) has been performed. The investigated case represents what would occur in a LOCA from the time the fuel is uncovered (DNB) until the re-flood occurs.

It was assumed that a reactor SCRAM occurs, but that the decay heat (~ 6% of the nominal reactor power) is deposited in the fuel and that there is no heat transfer from the fuel rod (adiabatic conditions) during this time. With a heat capacity of the fuel rod assumed to be 3.0 J/cm<sup>3</sup>/K, this gives a 400 K/min. rise in temperature. It is assumed that a core re-flood is established with 30 to 60 seconds, allowing the heat to be effectively removed.

The response of the coating layer stress at the end of the irradiation in a particle that has the reference coating thicknesses is shown for this transient in Figure 23. The tangential stress in the SiC layer becomes tensile with a stress magnitude of around 85 MPa for a temperature increase of 200 K ( $T_{\text{ker}}=1100$  K) with a resulting failure fraction of  $6.9 \times 10^{-4}$ . For a temperature increase of 400 K the resulting stress and failure fraction are, 188 MPa and  $3.5 \times 10^{-2}$ . If the statistical variation of the buffer and the SiC layer thicknesses is taken into account an average failure fraction (expected failed per total TRISO) of  $4.4 \times 10^{-2}$  is calculated, assuming a standard deviation of the thickness of 5  $\mu\text{m}$ .

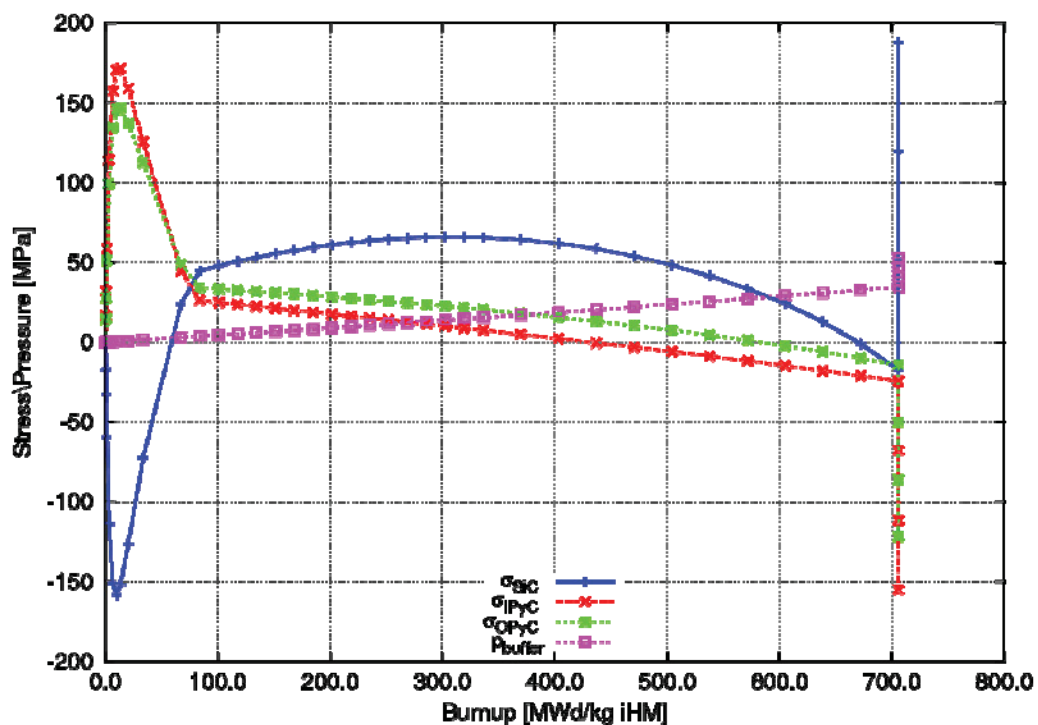


Figure 23. Coating stresses for a particle that experiences a LOCA transient at the end of its life-time in which the temperature of the particle is increased with 400 K.

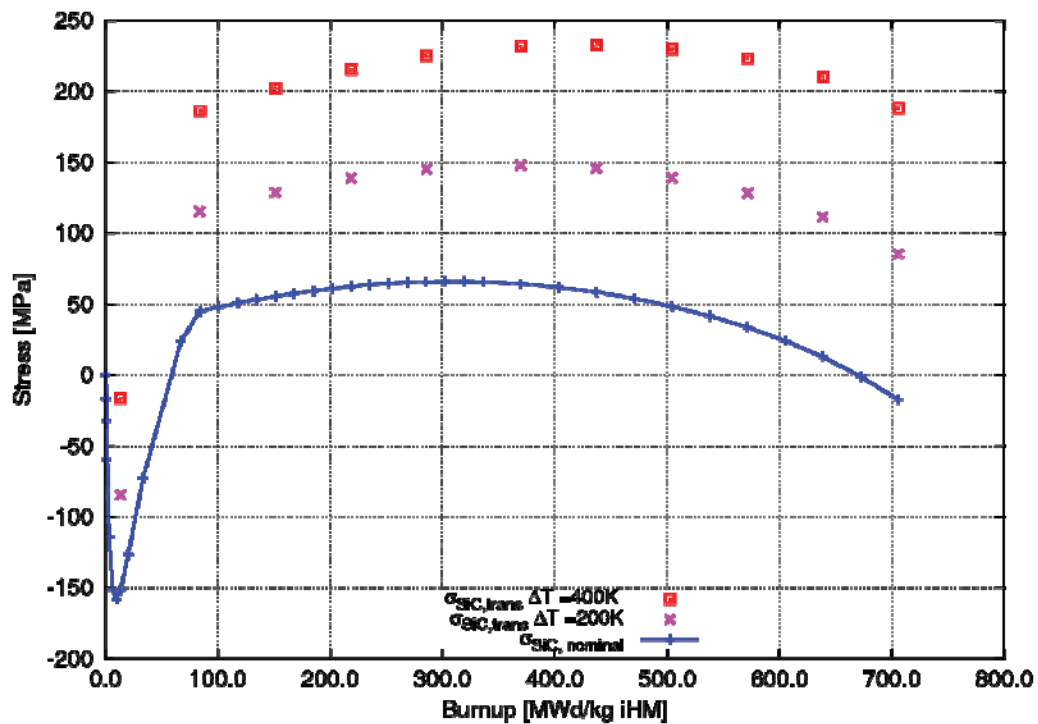


Figure 24. SiC-coating stresses for a particle that experiences a LOCA transient for various points in its life-time both a temperature increase of 200 K and of 400 K.

---

It can be seen from Figure 23 that the highest SiC stress level during normal operation does not occur at the end of the irradiation, but at a burnup of  $\sim 300$  MWd/kg. Therefore, the highest stress for the transient case could also occur at a lower burnup than the discharge burnup. Therefore, the impact of a LOCA on the fuel performance has been investigated for several burnup levels. The results are given in Figure 24. It can be seen from this figure that for a temperature increase of 200 K the highest SiC-coating stress level ( $\sim 150$  MPa) occurs at a burnup level of about 400 MWd/kg. This would result in a failure fraction of  $1.0 \times 10^{-2}$ . For a temperature increase of 400 K a failure fraction of  $1.0 \times 10^{-1}$  has been calculated.

The latter failure fractions have been calculated assuming a FGR fraction of 100 % during both normal operation and the transient. If a 'best-estimate' FGR fraction of 50 % is adopted the failure probability would be reduced to  $6.4 \times 10^{-4}$  and  $1.6 \times 10^{-2}$  for a temperature increase of 200 K and 400 K, respectively.

## 8. CONCLUSIONS

The performance of the FCM coated particle fuel has been analyzed under LWR-DB conditions. To allow for this analysis the following updates have been made to the PASTA code:

- The input routines have been updated to allow for automatic use of the neutronic data (burnup, fast fluence as a function of the irradiation time) that is generated with the DRAGON code. Furthermore, an input option for automatic evaluation of a temperature increase during anticipated transients (such as anticipated during a LOCA) has been added to the code.
- The thermal model in the code has been updated for calculation of temperatures of coated particles in a cylindrical pellet.
- Updated correlations for the PyC dimensional change under irradiation have been implemented in the code. The correlations, which are based on extrapolation of existing data, allow for the prediction of dimensional changes at high fluence levels that are expected for the FCM fuel.

The following observations have been made from the analyses obtained with the updated PASTA code for FCM fuel under normal operating and accident conditions:

- As was found in previous calculations the stress levels in the SiC-coating are low in general for low FGR fractions of several percent, which are based data of fission gas diffusion in UO<sub>2</sub> kernels. However, taking in mind the high burnup level of LWR-DB fuel, the FGR fraction is more likely to be in the range of 50 -100 %, similar to Inert Matrix Fuels. For this range the predicted stresses and failure fractions of the SiC-coating are high for the reference particle design (500 μm kernel diameter, 100 μm buffer, 35 μm IPyC, 35 μm SiC, 40 μm OPyC). A conservative case in which the FGR fraction was assumed to be 100 %, the fuel temperature 900 K and the fuel burnup of 705 MWd/kg (77 % FIMA) results in a failure probability of  $8.0 \times 10^{-2}$ . For a 'best-estimate' FGR-fraction of 50 % and a more modest burnup target level of 500 MWd/kg the failure probability drops below a value of  $2.0 \times 10^{-5}$ , which is the typical performance of TRISO fuel made under the German HTR research program of the past [26].
- In an optimization study on the particle design it was found that the performance can be improved if the buffer size is increased from 100 μm to 120 μm, while reducing the OPyC layer. The presence of the latter layer does not provide much benefit at high burnup levels (and fast fluence levels). Normally the shrinkage of the OPyC would result in a compressive force on the SiC-coating, which is advantageous. However, at high fluence levels the shrinkage is expected to turn into swelling, resulting in the opposite effect. This situation is however different when the SiC-matrix, in which the particles are embedded, is also considered in the analysis. In that case, the OPyC swelling can result in a positive effect (compressive force on the SiC-coating), since outward displacement of the OPyC outer surface is inhibited by the presence of the SiC-matrix. Taking some credit for this effect by adopting a 5 μm, SiC-matrix layer, the optimized particle (100 μm buffer and 10 μm OPyC), gives a failure probability of  $1.9 \times 10^{-4}$  for conservative conditions.
- During a LOCA transient, assuming a core re-flood in 30 seconds, the temperature of the coated particle can be expected to be about 200 K higher than the nominal temperature of 900K. For this event, the particle failure fraction for a conservative case (100 % FGR) was  $1.0 \times 10^{-2}$ , for the optimized particle design. For a FGR-fraction of 50 % this value reduces to  $6.4 \times 10^{-4}$ .

In general it can be concluded that a design modification of the reference particle design is desirable. The reference particle design exceeds the limiting failure fraction of  $2.0 \times 10^{-5}$  at a burnup level of 300

---

MWd/kg (assuming conservative conditions). To achieve higher burnup levels without exceeding this limit a modification of the design is necessary. This modified particle design would entail a larger buffer (>120  $\mu\text{m}$ ), which could be combined with a smaller OPyC coating (10  $\mu\text{m}$ ).

The next section provides several recommendations regarding experimental and modeling work necessary to reduce the uncertainty in the data used for the mechanical properties of the coating layers.

## **9. RECOMMENDATIONS FOR EXPERIMENTAL WORK REGARDING THE PERFORMANCE OF FCM FUEL**

To allow for future deployment of FCM fuel the following topics, in order of importance, are recommended for further investigation by computer modeling and experimental work:

### **1. Dimensional change and creep of PyC material**

From a literature survey it was found that experimental data regarding the dimensional change and creep under radiation of PyC is relatively scarce. For neutron fluence levels between  $8.0 \times 10^{21}$  and  $30 \times 10^{21} \text{ cm}^{-2}$  ( $E > 0.1 \text{ Mev}$ ), which are relevant for FCM fuel, there is no data available in literature. An experimental program for the quantification of PyC dimensional change is therefore highly recommended.

### **2. Fission gas release from the FCM kernel**

In comparison with HTR TRISO fuel kernels, the irradiation conditions of the FCM fuel kernel are very different. The temperature of the kernel is lower ( $T_{\text{max,FCM}}=900\text{K}$ ,  $T_{\text{max,HTR}}= 1500 \text{ K}$ ), while the maximum attained fluence levels are higher ( $\Phi_{\text{max,FCM}}=30 \times 10^{21} \text{ cm}^{-2}$ ,  $\Phi_{\text{max,HTR}}= 8.0 \times 10^{21} \text{ cm}^{-2}$ ). The first would typically result in a lower fission gas release from the kernel, while the latter might induce a high fractional release. Furthermore, the FCM fuel kernel contains a SiC-getter, which could ‘immobilize’ the fission gases resulting in a reduced fission gas release fraction.

It is unclear whether the combined effects would result in a higher or lower FGR as compared to typical HTR fuel kernels. Experimental work regarding FGR is key for the determination of the fuel performance of FCM fuel.

### **3. Mechanical integrity of the OPyC coating layer and SiC-matrix**

In the stress analysis it was found that the presence of the SiC-matrix can induce high stresses in the coating layers of the particle due to dimensional change of the OPyC layer. This phenomenon is not encountered in HTR TRISO fuel, since in that case a ‘softer’ graphite-matrix is used. It is therefore recommended that in a possible future irradiation experiment of FCM fuel, that the coated particles are embedded in a SiC-matrix.

Furthermore, the packing fraction of FCM is high (~44%) as compared to HTR fuel. Therefore, a given particle will have one or more neighboring particles within close proximity. This could induce further stress effects. It is therefore of key importance that the FCM coated fuel particles are embedded in a SiC-matrix during a future irradiation campaign.

Next to the experimental work itemized above, the incorporation in the PASTA code of the updated correlations and a re-evaluation of the fuel performance is recommended.

The following topics, in order of importance, are recommended for further investigation by computer modeling:

### **4. Impact of the SiC-matrix and neighboring particles on the coating stress**

Modeling of three-dimensional stress effects by neighboring particles and SiC-matrix to quantify the impact on the fuel performance is recommended. The results of 3D (finite element) modeling of coated particle fuel in matrix material could be used to update the boundary conditions of the (1D) stress analysis in PASTA. Next to this modification direct coupling with another code,

---

typically a finite element code, such as BISON [27], would also allow for the evaluation of matrix effects. In any case, three-dimensional modeling of coated particle fuel in matrix material is recommended.

**5. Coupling of the PASTA code with fuel performance model for pin-type fuel**

In order to treat the entire fuel geometry (coated particle, pellet, gap, cladding) the PASTA code could be coupled to fuel performance codes that are dedicated to pin-type fuel, such as TRANSURANUS [28] or FRAPCON [29]. This would allow for the re-evaluation of the current envisaged FCM pin-type fuel.

**6. Consideration of helium in gas release from fuel kernels**

In cases where significant quantities of minor actinides (especially curium) are present either at beginning of irradiation or during irradiation, helium produced by alpha decay can be substantial. This should be quantified in future work.

## REFERENCES

- [1] Versluis, R. M., Venneri, F., Petti, D., Snead, L., and McEachern, D., 2008, "Project Deep-Burn: Development of Transuranic fuel for High-Temperature Helium-Cooled Reactors," Proc. of the 4<sup>th</sup> International Topical Meeting on High Temperature Reactor Technology (HTR2008), Washington DC, USA.
- [2] G. L. Bell, L. L. Snead, R. D. Hunt, J. H. Miller, T. M. Besmann, and J.D. Hunn, 2010, "Development of TRU TRISO Fuel for Deep Burn", 11th Information Exchange Meeting On Actinide and Fission Product Partitioning and Transmutation, San Francisco, California.
- [3] B. Boer, A. M. Ougouag, J.L. Kloosterman, G.K. Miller, 2008, "Stress Analysis of Coated Particle Fuel in Graphite of High-Temperature Reactors", *Nuclear Technology*, **162**, p. 276-292.
- [4] G. Sengler, F. Forêt, G. Schlosser, R. Lisdat, S. Stelletta, 1999, "EPR core design", *Nuclear Engineering and Design*, **187**, p. 79-119.
- [5] Marleau, G., A. Hébert, and R. Roy, 2010, "A User Guide for Dragon Version4," Technical Report IGE-294, École Polytechnique de Montréal.
- [6] B. Boer, A.M. Ougouag, 2011, "Final Report on Utilization of TRU TRISO Fuel as Applied to HTR Systems Part I: Pebble Bed Reactors", INL/EXT-11-21436, FCRD-FUEL-2011-000062.
- [7] J.C. Maxwell,-Garnett. Phil. Trans. Roy. Soc. Lond., A 203, p. 385, 1904.
- [8] J.J. Duderstadt and L.J. Hamilton, 1976, "Nuclear Reactor Analysis", pp. 475-482.
- [9] D. Olander, "Fundamental Aspects of Nuclear Reactor Fuel Elements", 1976.
- [10] D.G. Martin, "Considerations Pertaining to the Achievement of High-Burnups in HTR Fuel," *Nuclear Engineering and Design*, 213, pp. 241-258, 2001.
- [11] L.L. Snead, et al., 2007, "Handbook of SiC properties for fuel performance modeling", *Journal of Nuclear Materials*, **371**, p. 329-377.
- [12] J.L. Kaae, D.W. Stevens, J.C. Bokros, 1972, "Dimensional changes induced in poorly crystalline isotropic carbons by irradiation", *Carbon*, **10**, p. 561-570.
- [13] B.T. Kelly et al., "Irradiation Damage in Graphite due to Fast Neutrons in Fission and Fusion Systems", IAEA Tecdoc 1154, April 2000.
- [14] P.DeMange, J. Marian, M. Caro, A. Caro, 2010, "TRISO-fuel element thermo-mechanical performance modeling for the hybrid LIFE engine with Pu fuel blanket", *Journal of Nuclear Materials*, **405**, p. 144-155.
- [15] F. Ho, "Material Models of PyroCarbon and Pyrolytic Silicon Carbide", CEGA-002820, 1993.
- [16] J.L. Kaae, "The mechanical behavior of BISO-coated fuel particles during irradiation. Part 1: Analysis of stresses and strains generated in the coating of a BISO fuel particle during irradiation", *Nuclear Technology*, **35**, p.359-367, 1977.
- [17] J. Jonnet, J.L. Kloosterman and B. Boer, "Development of a stress analysis code for TRISO particles in HTRs", *International Conference on the Physics of Reactors, Nuclear Power: A Sustainable Resource*, Switzerland (2008).
- [18] J.M. Smith, H.C. Van Ness, M.M. Abott, 2005, "Introduction to Chemical Engineering Thermodynamics".



- [19] B. Boer and A.M. Ougouag, 2010, "Stress analysis of coated particle fuel in the Deep-Burn pebble bed reactor design", *PHYSOR 2010 - Advances in Reactor Physics to Power the Nuclear Renaissance, Pittsburgh, Pennsylvania, USA, May 9-14, 2010, on CD-ROM, American Nuclear Society, LaGrange Park, IL.*
- [20] A. Hébert, 1993, "A Collision Probability Analysis of the Double-Heterogeneity Problem," *Nuclear Science and Engineering*, **115**, No. 2, p. 177.
- [21] N. Hfaiedh, A. Santamarina, 2005, "Detemination of the Optimized SHEM Mesh for Neutron Transport Calculations," *Proc. Mathematics and Computation, Supercomputing, Reactor Physics and Nuclear and Biological Applications*, Avignon, France.
- [22] M.A. Pope, B. Boer, A.M. Ougouag, G.Youinou, 2011, "Performance of Transuranic-Loaded Fully Ceramic Micro-Encapsulated Fuel in LWRs", Interim Report, Including Void Reactivity Evaluation", Idaho National Laboratory, INL/EXT-11-21343.
- [23] M. Barrachin, R. Dubourg, S. de Groot, M.P. Kissane, K. Bakker, 2011,"Fission-product behaviour in irradiated TRISO-coated particles: Results of the HFR-EU1bis experiment and their interpretation", *Journal of Nuclear Materials*, **415**, p. 104-116.
- [24] C. Degueldre and W. Wiesenack, 2008, "Zirconia Inert Matrix Fuel for Plutonium and Minor Actinide Disposition in Reactor and as Ultimate Waste Form", Proceedings of the Material Research Society spring meeting.
- [25] A.M. Ougouag, J.L. Kloosterman, W.F.G. van Rooijen, H.D. Gougar, W.K. Terry, 2006, "Investigation of bounds on particle packing in pebble-bed high temperature reactors", *Nuclear Engineering and Design*, **236**, p. 669-676.
- [26] K.Verfondern, W. Schenk, H. Nabielek, 1990, "Passive Safety characteristics of fuel for a modular HTR and fuel performance modeling under accident conditions", *Nuclear Technology*, **91**, p. 235.
- [27] C. Newman, G. Hansen, and D. Gaston. 2009, "Three dimensional coupled simulation of thermomechanics, heat,and oxygen diffusion in UO<sub>2</sub> nuclear fuel rods", *Journal of Nuclear Materials*, **392**, p. 6-15.
- [28] K. Lassmann, 1992, "TRANSURANUS: a fuel rod analysis code ready for use", *Journal of Nuclear Materials*, **188**, p. 295-302.
- [29] G.A. Berna, C.E. Beyer, K.L. Davis, D.D. Lanning, 1997, "FRAPCON-3: A computer code for the calculation of steady-state thermal-mechanical behavior of oxide fuel rods for high burnup", NUREGKR-6534, Vol. 2, PNNL-11513.